Eastward Flow through the Mid-Atlantic Ridge at 11°N and Its Influence on the Abyss of the Eastern Basin*

M. S. MCCARTNEY

Department of Physical Oceanography, Woods Hole Oceanographic Institution, Woods Hole, Massachusetts

S. L. BENNETT

Northwest Hydraulic Consultants, North Vancouver, British Columbia, Canada

M. E. WOODGATE-JONES

Department of Physical Oceanography, Woods Hole Oceanographic Institution, Woods Hole, Massachusetts

(Manuscript received 26 January 1990, in final form 14 December 1990)

ABSTRACT

The dilute Antarctic Bottom Water of the North Atlantic eastern trough is supplied from the western trough through fractures in the Mid-Atlantic Ridge. In particular, the influence on eastern trough property distributions of flow through the Romanche and Vema fracture zones, near the equator and 11°N, respectively, has been noted previously.

Here, new observations are reported that document the abyssal circulation of the northeastern Atlantic basins (Gambia Abyssal Plain, South Canary Basin, and North Canary Basin) in particular, the dominance of Vema influence, the absence of Romanche influence, and the existence of a system of deep western boundary currents and estimated transports.

Deep isopycnals slope steeply across the Vema's eastern end near 39°W, corresponding to a geostrophic transport through the Vema of 2.1 to 2.3 ($\times 10^6$ m^3 s^{-1}) colder than 2.0°C. This is half or more of the estimated Bottom Water that flows north across the equator into the subtropical western North Atlantic.

This transport in the Vema debouches into the Gambia Abyssal Plain. A deep western boundary current with 1.3 to 3.0 ($\times 10^6$ m^3 s^{-1}) transport colder than 2.0°C flows eastward. This current subsequently bifurcates into 1) a nearly zonal eastward current ($\leq 1.0 \times 10^6$ m^3 s^{-1} transport) along the plain's southern boundary, the Sierra Leone Rise, and 2) a northward western boundary current along the flank of the Mid-Atlantic Ridge (1.8 to 3.9 $\times 10^6$ m^3 s^{-1} transport).

Property and shear fields indicate that, for water colder than 2.0°C, basically none of the eastward flow along the rise passes southward through its deepest passage, the Kane Gap, nor does Romanche-derived water flow north there. The poleward Mid-Atlantic Ridge flank flow in the plain continues northward across the Cape Verde Ridge into the South Canary Basin and from there poleward into the North Canary Basin.

1. Introduction

By the 1930s, sufficient abyssal water mass measurements and depth soundings in the North and South Atlantic had accumulated for Wüst (1933, 1935) to construct charts and sections of deep and bottom waters and to infer circulation pathways and topographic constraints from them. In the western trough, he found western-intensified Weddell Sea influence (later named "Antarctic Bottom Water" or simply "Bottom Water") spreading northward from the Antarctic zone as far as the northern subtropics. Along the spreading path, he found the coldest bottom potential temperature θ_B increasing steadily northward, from < -0.8°C immediately north of the Weddell Sea, to +0.6°C at the equator, and finally to +1.8°C near Bermuda.

In the eastern trough, Wüst found a different bottom water configuration, with the coldest bottom temperatures[1] located near the equator and bottom temperatures increasing from equator to pole in both hemispheres. Wüst (1933) attributed this to eastward flow through the Romanche Fracture Zone, followed by poleward spreading. Later studies (Metcalf et al. 1964) confirmed the presence of cold water in the Ro-

* Woods Hole Oceanographic Institution Contribution Number 5858.

Corresponding author address: Dr. Michael S. McCartney, Dept. of Physical Oceanography, Woods Hole Oceanographic Institution, Woods Hole, MA 02543.

[1] All temperatures in this paper are potential temperatures.

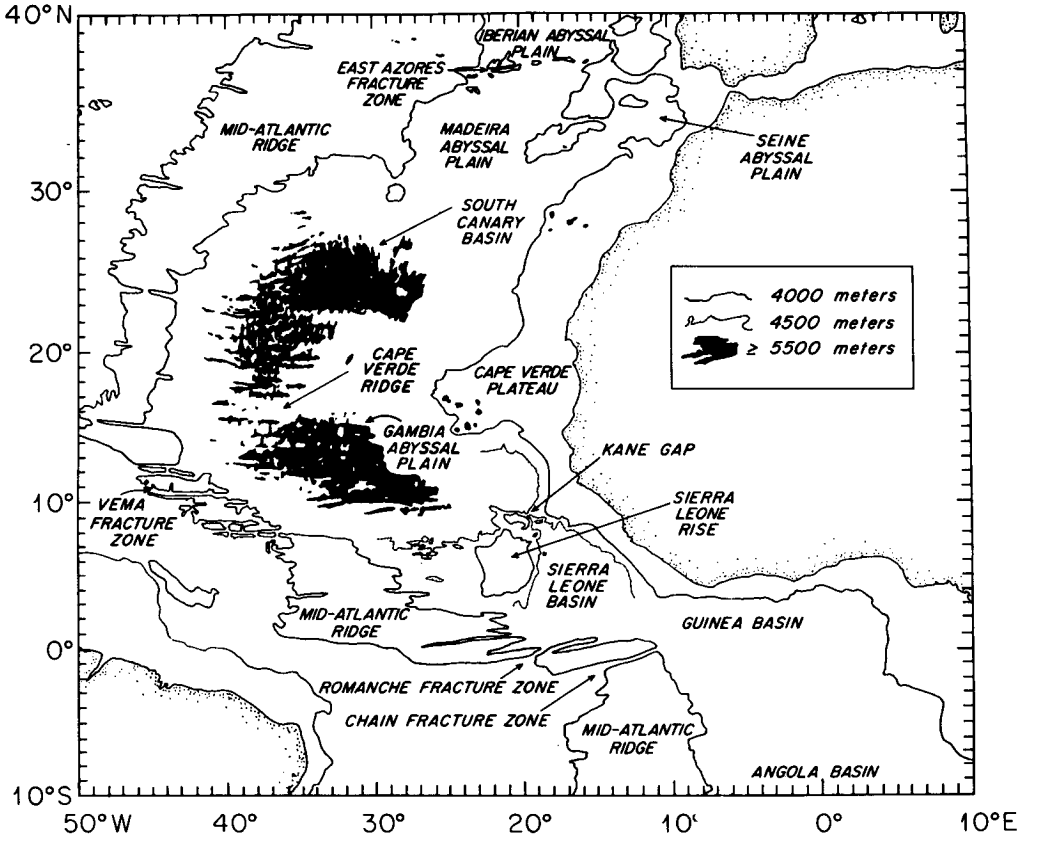

FIG. 1. A lexicon of names for bottom topography features in the eastern trough of the Atlantic Ocean, and selected isobaths from the GEBCO topography charts (Searle et al. 1982).

manche and its influence on the abyssal water of the Guinea and Sierra Leone basins of the equatorial and southeastern Atlantic (Fig. 1 shows regional bathymetry and bathymetry names). Hobart et al. (1975) reported distinctly warmer water at the sill of the Kane Gap, the deepest passage from the Sierra Leone Basin north to the Gambia Abyssal Plain.

A second eastward flow through the Mid-Atlantic Ridge, near 8°N and weaker than that through the Romanche, was later suggested by Wüst (1935) based on new depth soundings and observations of an isolated θ_B minimum east of the ridge at 12°N (θ_B = 1.74°C at *Meteor* station 305 near 34°W). Heezen et al. (1964) later described seven fractures between 7° and 13°N, including one at 8°N, Wüst's preferred location. The deepest of Heezen et al.'s fractures is the Vema Fracture Zone at 11°N; they inferred an approximate depth (4500 m) and location for its sill from a west-to-east jump in θ_B across 41°W, which was later confirmed and sharpened by the Seabeam bathymetric survey of Vangriesheim (1980).

Since Wüst's time, the relative impact of Vema and Romanche fracture zones' flows on the eastern trough has remained unclear, despite the accumulation of new hydrographic and bathymetric data. The Worthington and Wright (1970) atlas [based on the earliest Atlantic data with salinometer salinity determinations, the IGY data (summarized by Fuglister 1960) plus a few additional 1960s stations] shows an isolated pool of cold water ($\theta_B \leq 1.8$°C) over the Gambia Abyssal Plain, but does not resolve its connection path to the western trough parent water mass (Fig. 2a). At the next temperature boundary, $\theta \leq 1.9$°C, they indicated a connection of this pool south through the Kane Gap to the Sierra Leone Basin, inferred from the 8°N IGY section (Fuglister 1960) that passes just south of the Kane Gap sill. The broad goal of the program we undertook in the early 1980s was to examine the alternative possibility of the Vema Fracture Zone being the principal connection path from the western trough to the Gambia Abyssal Plain.

In a comprehensive review of the world ocean's deep circulation, Warren (1981) wrote:

> . . . the principal inflow of water below the general crest of the Mid-Atlantic Ridge (3500 m depth, say) occurs from the western Atlantic through the Romanche Fracture Zone on the equator (e.g., Drygalski, 1904; Wüst, 1933; Metcalf, Heezen, and Stalcup, 1964). No estimate of the rate of this inflow has been made. Silica values on the surface where potential

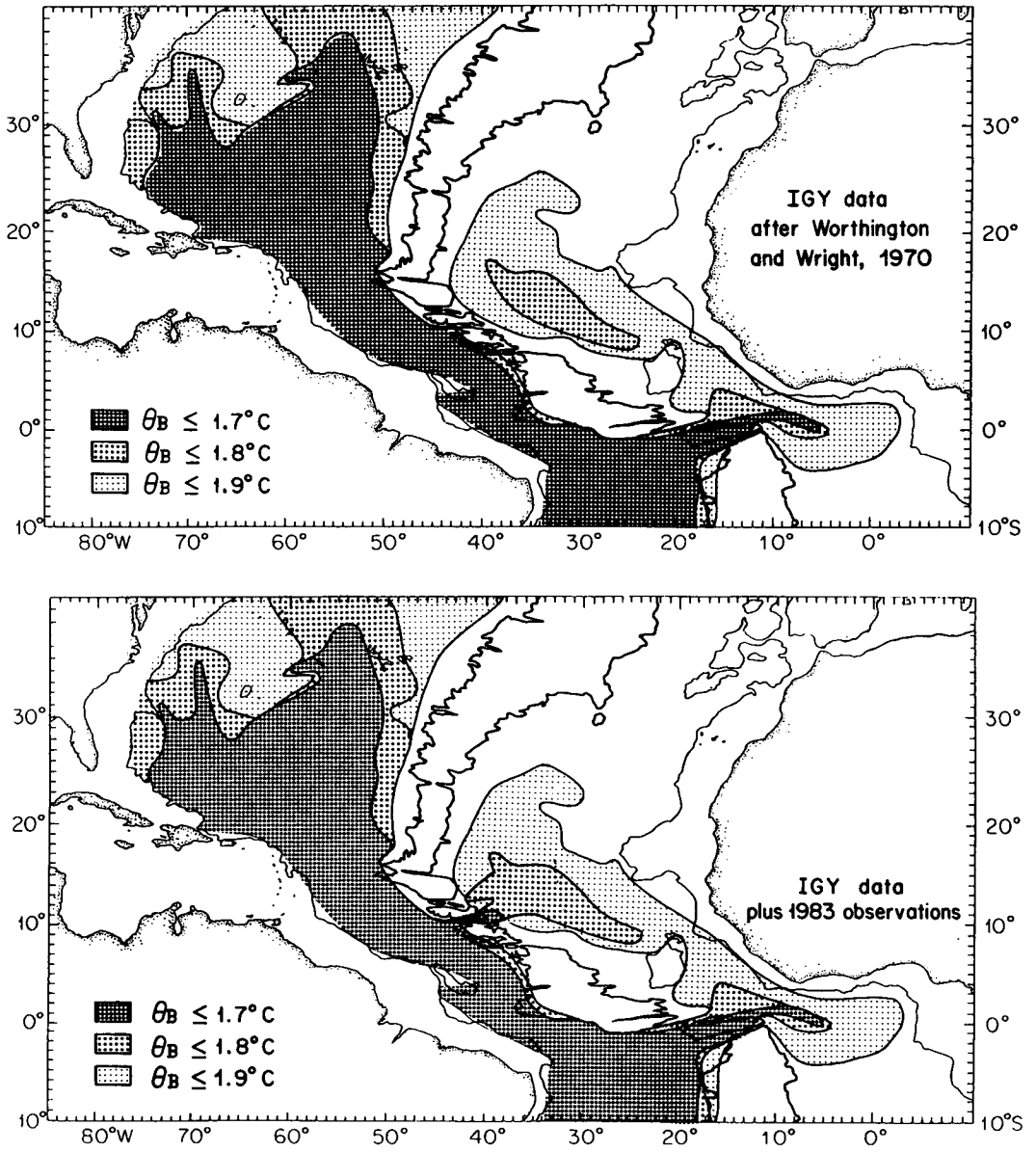

FIG. 2. Derived from Worthington and Wright (1970). The shadings delimit the regions where the near-bottom potential temperature is colder than the indicated value. (a) Data limited to the early high-precision salinity datasets (salinometer-based). As contoured by Worthington and Wright. (b) Modification indicated by the present study.

temperature is 2°C increase northward (Metcalf 1969), as well as southward (Chan, Drummond, Edmond and Grant, 1977), indicating further that the deep water "ages" poleward. Many additional fracture zones cut across the Mid-Atlantic Ridge, but the existing evidence suggests that there are only three others through which noticeable deep water transport may take place . . . Indications of eastward flow through the Vema Fracture Zone near 11°N were shown by Heezen, Gerard, and Tharp (1964), but the flux must be much less than that through the Romanche Fracture zone, given its much smaller influence on property distributions in the eastern Atlantic . . .

In contrast, Mantyla and Reid (1983), drawing on much the same literature and data as Warren and writing only a couple of years later, say:

> Evidently, the Romansche Gap is the primary passage for bottom water flow into the eastern equatorial and southeastern Atlantic Basins, while the Vema Fracture Zone is the main passage for bottom water flow into the northeastern Atlantic basins.

Another matter for debate has been the existence of deep western boundary currents in the northeastern Atlantic basins (specifically the Gambia Abyssal Plain,

the South Canary Basin, and the North Canary Basin). Of this area, Warren (1981) states:

> The dynamical fact that poleward movement from an equatorial source can be accomplished by an interior flow may explain to some extent why no deep boundary currents along the western margin of the eastern trough (Mid-Atlantic Ridge) have been observed in transatlantic sections (Fuglister, 1960). On the other hand . . . the budgetary function of western boundary currents is not only to transport deep water into low latitudes, but also to correct imbalances between interior flows and upward fluxes; and it is not easy to see how continuity can be maintained in the eastern trough of the Atlantic without recirculation boundary currents.

The new high-quality CTD hydrographic transects reported here (Fig. 3)—part of a set whose collection began while Warren and Mantyla and Reid were writing their reviews—in large measure settle the question of the relative importance of Romanche and Vema flow on the abyssal characteristics of the eastern trough. The new data rather firmly support Mantyla and Reid's inference that eastward flow through the Vema Fracture Zone is the dominant influence governing the water mass characteristics of the abyssal northeastern Atlantic basins. The Gambia Abyssal Plain is extensively overlain by waters from the Vema, at some locations exceeding 1000 m thickness. The isolated cold pool over the Gambia Abyssal Plain in the Worthington and Wright (1970) charts (Fig. 2a) thus is connected through the Vema Fracture Zone to the cold water of the western trough, as sketched in Fig. 2b. Romanche-derived water is not evident north of the Kane Gap. The new data also document the northeastern Atlantic basins' deep circulation, including their deep boundary currents (Fig. 4). The flow exiting the Vema supplies a cyclonic circulation over the Gambia Abyssal Plain, which, in turn, supplies a northward flow across the Cape Verde Ridge to the Canary Basin. This northward flow is western-intensified over the ridge and in the Canary Basin.

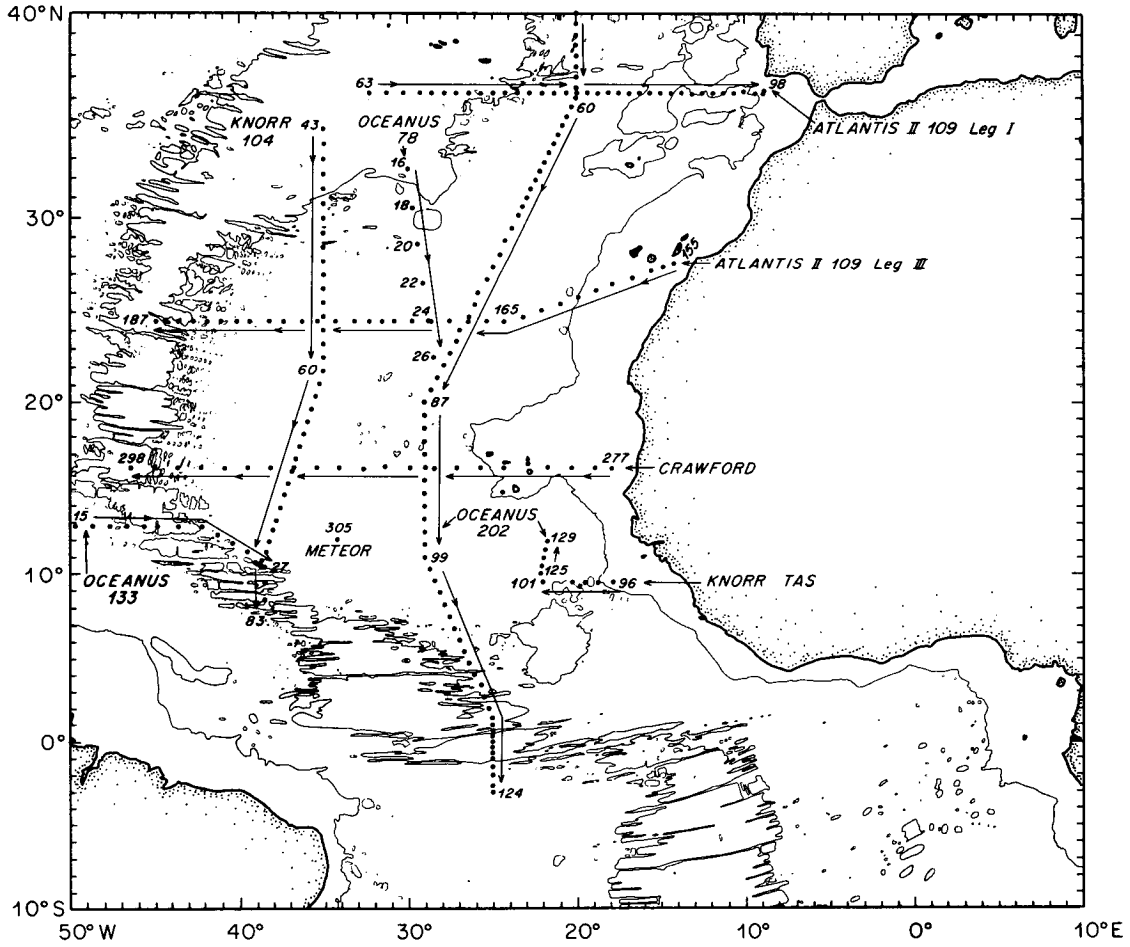

FIG. 3. Locations of principal CTD station lines and other data explicitly used in this study. WHOI computer bathymetry database.

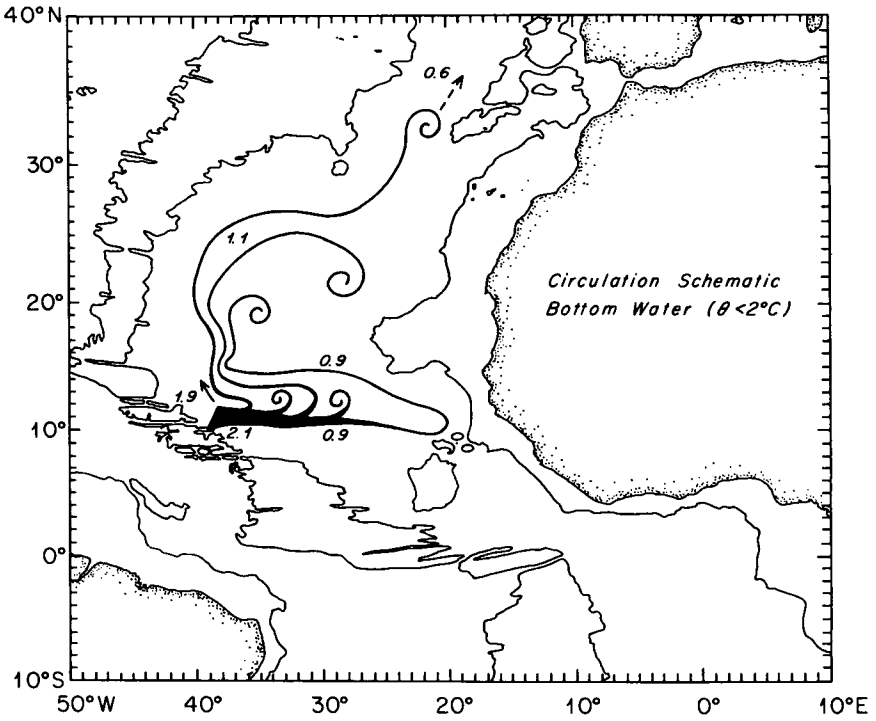

FIG. 4. Circulation schematic for the cold (≤2.0°C) Bottom Water debouching the Vema Fracture Zone into the northeastern Atlantic basins. Numbers are transport estimates in 10^6 m^3 s^{-1}, for an isothermal reference level of 2.2°C. The flow axes are estimated from bottom temperatures (Fig. 13b) and pass through station groups used for the transport estimates. The axes widths are not significant. The curled tips indicate flow across the 2.0° isotherms. The dashed arrow is the transport of 2.0° to 2.05°C water across 36°N.

2. The Vema Fracture Zone

a. Early observations

1) DISCOVERY OF THE VEMA FRACTURE ZONE AND PRIMARY SILL

Heezen et al. (1964) observed that a succession of fracture zones offsets the Mid-Atlantic Ridge axis progressively westward in the northern tropics. They noted that these fractures are easily recognized in echo-sounding transects because they are floored by extensions of the western trough abyssal plain: returns from the flat floors stand out from the generally noisy background signal of the rough ridge topography. Heezen et al. proposed that Wüst's postulated low-latitude eastward leak of Bottom Water across the ridge occurs through the deepest of these tropical fractures, the Vema Fracture Zone at 11°N.

As Heezen et al. described, the Vema offsets the Mid-Atlantic Ridge axis west from roughly 41° to 43.5°W. The Demerara abyssal plain of the western trough extends eastward into the Vema to about 41°W with about 5200 m depth and 8 to 20 km width. The Vema's bounding scarps west of 41°W rise steeply above the floor by a few hundred to 3000 m. East of 41°W the distinguishing flat floor disappears, making their identification of the fracture in isolated transects more tentative, but with indications that the maximum depths there also exceed 5000 m. Their echo-sounding transects east of 41°W suggest that the bounding scarps deepen eastward, with the northern scarp descending more rapidly, dropping below 4500 m by about 38°W.

Heezen et al. inferred the existence of a sill between 41° and 40.5°W at approximately 4500 m depth, from a jump in near-bottom (about 5200 m) temperature between these two longitudes. At this depth, the same near-bottom temperature (1.27°C) was observed in the western trough and in the Vema at 41°W, while farther east in the Vema at 40.5°W a significantly higher temperature (θ = 1.48°C) was observed. This warmer temperature corresponds to the temperature at 4500 m depth and 41°W, thus their inference of a sill depth.

The inferred sill configuration was corroborated by a 1977 Seabeam survey (reported by Vangriesheim 1980; data collected by D. Needham). The sill is a triple one, with depths of 4690, 4650, and 4710 m (all ± 10 m), at 41°01'W, 40°55'W, and 40°53'W, respectively. The minimum observed sill depth is about 150 m deeper than the Heezen et al. estimate, and the observed near-bottom temperature immediately east of the sill

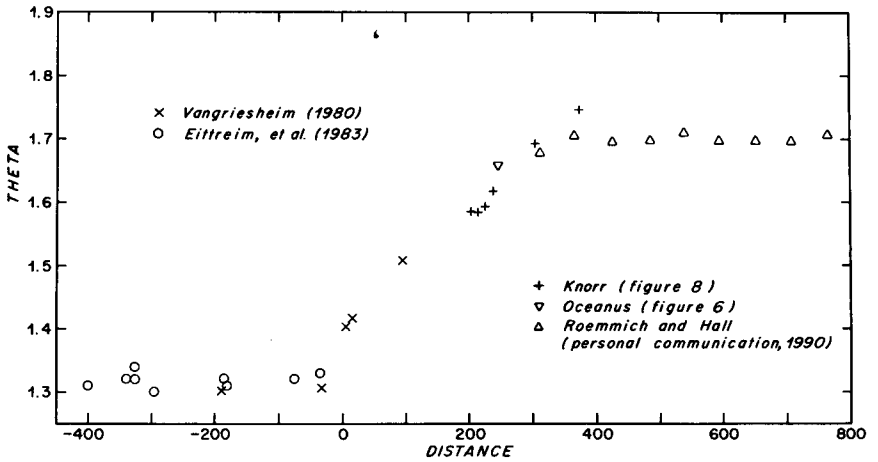

FIG. 5. Near-bottom temperature in the Vema Fracture Zone west of primary sill (distance < 0), east of primary sill (positive distance < 240 km), and in the eastern basin downstream of the exit sill.

correspondingly colder at 1.40°C. Considering the sparseness of temperature and echo sounding data on which it was based, the Heezen et al. inference was impressively accurate.

2) SECONDARY SILL AND DOWN-CHANNEL CHANGES IN BOTTOM TEMPERATURE

Heezen et al. speculated that the Vema also has a secondary sill, which would account for Wüst's observation of warmer (1.74°C) near-bottom temperatures nearby in the eastern trough than those downstream of the primary sill. Observed bottom temperatures in the Vema (shown in Fig. 5) evolve down-channel from a remarkably uniform value[2] west of the sill (1.30 to 1.34°C) to a sharply higher value just east of the primary sill (1.40°C). Proceeding eastward from there, temperatures warm at a rate of about 0.1°C per 100 km. The available bottom temperature observations by themselves do not reveal if the 0.1°C per 100 km warming east of the sill occurs gradually or in jumps at (an) additional sill(s). We present evidence below that Heezen et al.'s speculation regarding a secondary sill is essentially correct.

b. 1983 obervations

We first occupied seven CTD stations near the Vema in early 1983 while aboard the R/V *Oceanus,* after completing a 20-station transect of the western trough near 13°N. These seven stations cross the Mid-Atlantic Ridge eastward, then cross the Vema southeastward about 240 km east of the primary sill, following the ridge's eastern flank from 13° to 10°N (Fig. 3).

Very cold Bottom Water (θ_B = 1.66°C at 4800 m on station 26) was found, 0.08°C colder than Wüst's observation some 500 km farther east, at a station in a deep north of the Vema and separated from it by 4600 m topography (Fig. 6); the station missed the deep's maximum depth by at least 200 m. A station was not obtained in the maximum depths of the Vema, due to time restrictions and a deteriorating echo-sounding system between stations 25 and 27.

To investigate further the distribution and flow of Bottom Water near and through the Vema, we returned

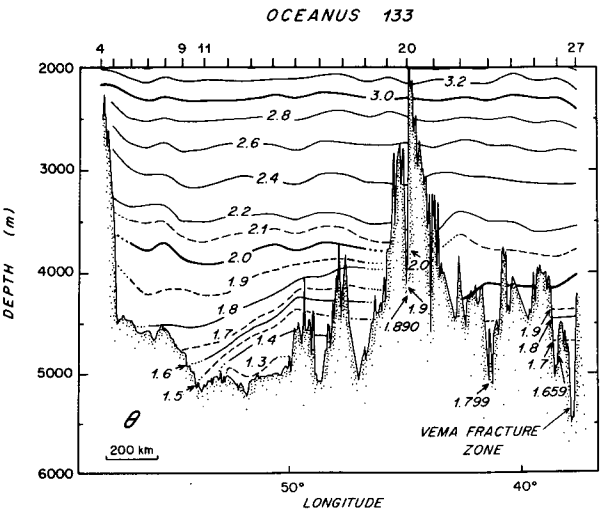

FIG. 6. The deep potential temperature distribution for a section between Barbados and the Mid-Atlantic Ridge along 12°30'N to station 22, and along the east flank of the ridge on a southeast course (station locations Fig. 3) across the Vema Fracture Zone.

[2] This illustrated range is warmer than the single Heezen et al. (1964) thermoprobe measurement west of the sill (1.27°C). This difference could reflect decadal warming or an accuracy limitation of the thermoprobe.

on the R/V *Knorr* during a north–south Atlantic transect near 35°W in late 1983, deflecting the cruise track to intersect the Vema near 38°30′W (Fig. 3). We first ran the *Knorr* on a triangular reconnaissance survey (Fig. 7a) of the Vema's eastern end; the only other bathymetric data at the time was a low-resolution chart (Searle et al. 1982). Without time for any real reflection, we placed a station (station 76) near the crest of the northern wall of the Vema in 4765 m depth, and worked a line of stations (Fig. 8) to the east-southeast across the floor of the Vema, which exceeds 5200 m at this longitude. The north wall descends sharply to the floor of the Vema, and our first station over the floor (77) exceeded the apparent echo sounding depth by over 860 m. Two more stations were made over the floor, and one part way up the less steep southern wall in 4630 m. The line then rejoins the primary transect at station 81, well up the Mid-Atlantic Ridge in 4240 m.

At this longitude the Bottom Water was found in a thick layer with low vertical gradients separated from the overlying Deep Water by a layer of strong gradients. Vangriesheim (1980) and Eittreim et al. (1983) found a similar structure farther west in the Vema, but at our location the near-bottom temperature is considerably warmer than at or west of the primary sill (Fig. 5). Temperature, σ_4, nitrate, and silicate sections are shown in Fig. 8. The bottom temperature at station 76 on the north wall in 4760 m was found to be as cold (1.58°C) as that at the floor of the Vema 600 m deeper. The coldest waters within the Vema at this longitude are thus escaping from the Vema over the northern wall at a depth near 4700 m. The cold water in the Vema is piled up against the north wall, as illustrated by the steeply sloped 1.6°C isotherm in Fig. 8. In the small region between our Vema section and the primary *Knorr* section farther north in the eastern trough there is a pathway exceeding 4700 m depth, indicating free access to the eastern trough of the waters passing over the north wall. This region then is the Heezen et al. secondary sill, which we will call the Vema exit sill. Our hydrographic section immediately upstream of this sill (Fig. 8) shows sloped isotherms consistent with geostrophic transport of water across the sill, and allowing a transport estimate. We consider first the details of the exit sill, second the implications of the downstream warming of the bottom temperature (Fig. 5), and third the estimation of transport.

1) VEMA EXIT SILL TOPOGRAPHY

The echo-sounding track between *Knorr* station 76 on the north wall of the Vema and station 75 in the eastern trough show depths exceeding 4700 m almost everywhere (Fig. 8). About 4 km northeast of station 76, a 2 km-wide shoal reached as shallow as 4580 m, and as we steamed east-southeast from station 76 across the floor of the Vema, another narrow shoal was crossed, rising above 4510 m before depths descended to the floor. On the basis of these data alone a sill between 4500 and 4600 m would be possible. But there are other bathymetric transects nearby that suggest that the deepest pathway between the *Knorr* stations over the Vema floor (77–79) and the open eastern trough (station numbers ≤ 75) exceeds 4700 m.

A specific trackline along 39°W (trackline B, Fig. 7a) shows the north wall cresting at 4739 m just north of our station 77, which has a temperature of 1.598°C at that depth. This trackline continues north past 11°N with depths exceeding 4739 m. A nearly zonal trackline along the north wall (Fig. 7b) shows a 14 km passage exceeding 4700 m (and as deep as 2768 m at two locations) at the intersection with the 39°W trackline, and a second broader passage to its east, reaching deeper than 4800 m at two locations. We include on this transect a ghost image of our Vema hydrographic section (Fig. 8) to illustrate the relationship of the isotherm depths within the Vema to the topography of this exit sill trackline. We include the 1.659°C isotherm, as this was the near-bottom temperature observed at our *Oceanus* station 26 north of the north wall. Also recall from Fig. 5 that the Roemmich and Hall section along 11°12′N shows an extensive region of temperatures just colder than 1.7°C extending east from 38°14′W. The superposition of the isotherms and the north wall bathymetry show that within the Vema well above the floor at the depth of the sill immediately to the north, temperatures are as cold as those at the bottom north of the sill. Together these data lend credence to the idea that the coldest temperature north of the north wall can be well estimated from the projection of the sill depth onto the temperature profile south of the north wall. After completion of this exit sill discussion we will return to the question of the relationship of the temperature structure upstream and downstream of a sill.

Figure 7c is the contouring of the exit sill topography using the tracklines indicated in Fig. 7a. The data come from several sources: our own *Knorr* and *Oceanus* cruises, a later *Oceanus* track at 11°12′N (Roemmich and Hall, personal communication 1990), and a Lamont–Doherty Geological Observatory database (D. Martinson, personal communication 1986). The indicated quasi-zonal trackline on Fig. 7a was rejected as totally inconsistent with the rest of the data. The cross-over disagreements of the remainder of the tracklines reflect navigation uncertainties of a few miles at most and are thus contourable with minimal smoothing. For clarity only three depth contours are shown: 4500 m to define walls and bounding scarps that penetrate through the Bottom Water and thus confine it; 5000 m to define the principal deeps extending west into this region from the eastern trough and the Vema deep penetrating east into the region from the west; and 4700 m to define the possible path-

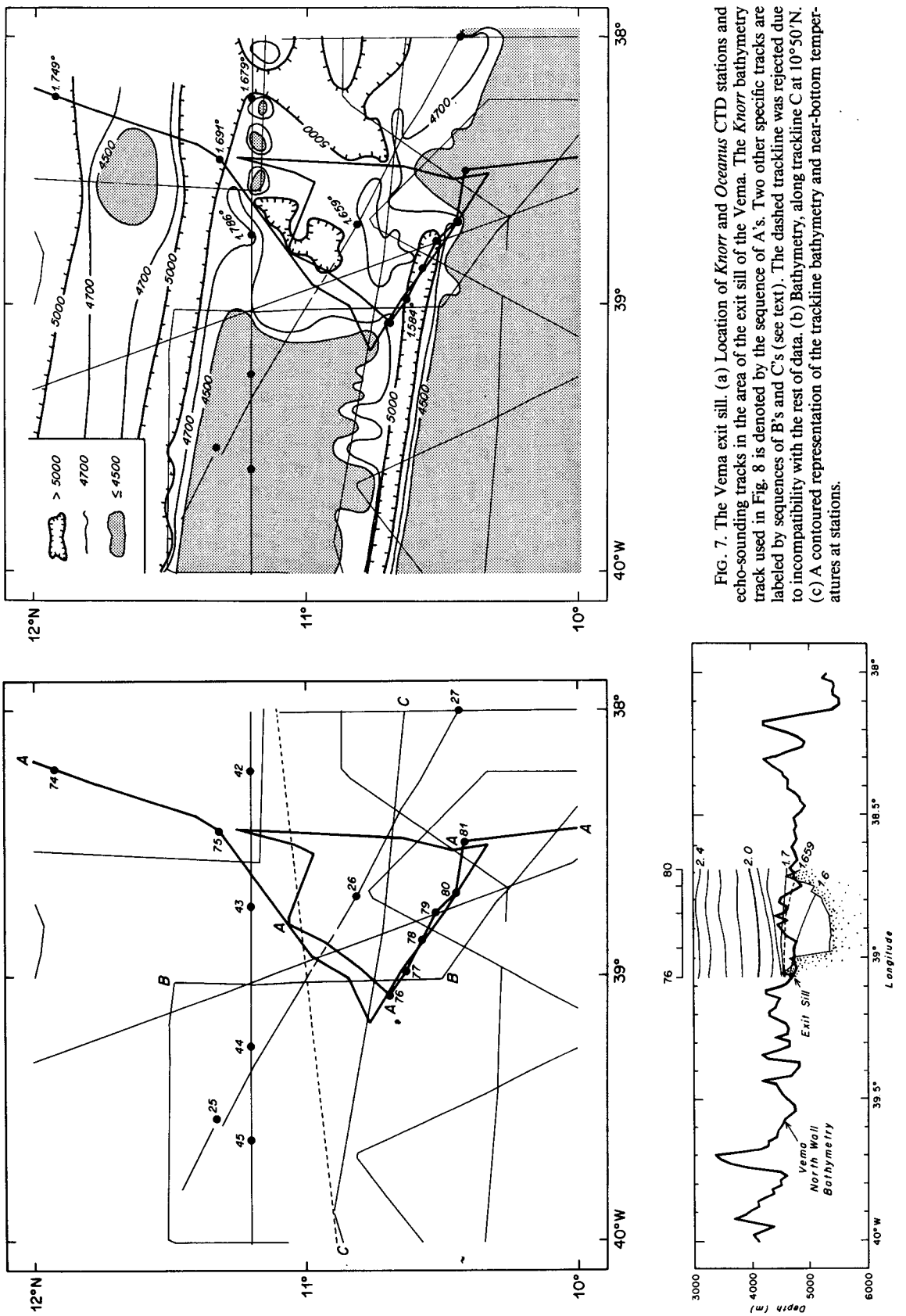

FIG. 7. The Vema exit sill. (a) Location of *Knorr* and *Oceanus* CTD stations and echo-sounding tracks in the area of the exit sill of the Vema. The *Knorr* bathymetry track used in Fig. 8 is denoted by the sequence of A's. Two other specific tracks are labeled by sequences of B's and C's (see text). The dashed trackline was rejected due to incompatibility with the rest of data. (b) Bathymetry, along trackline C at 10°50'N. (c) A contoured representation of the trackline bathymetry and near-bottom temperatures at stations.

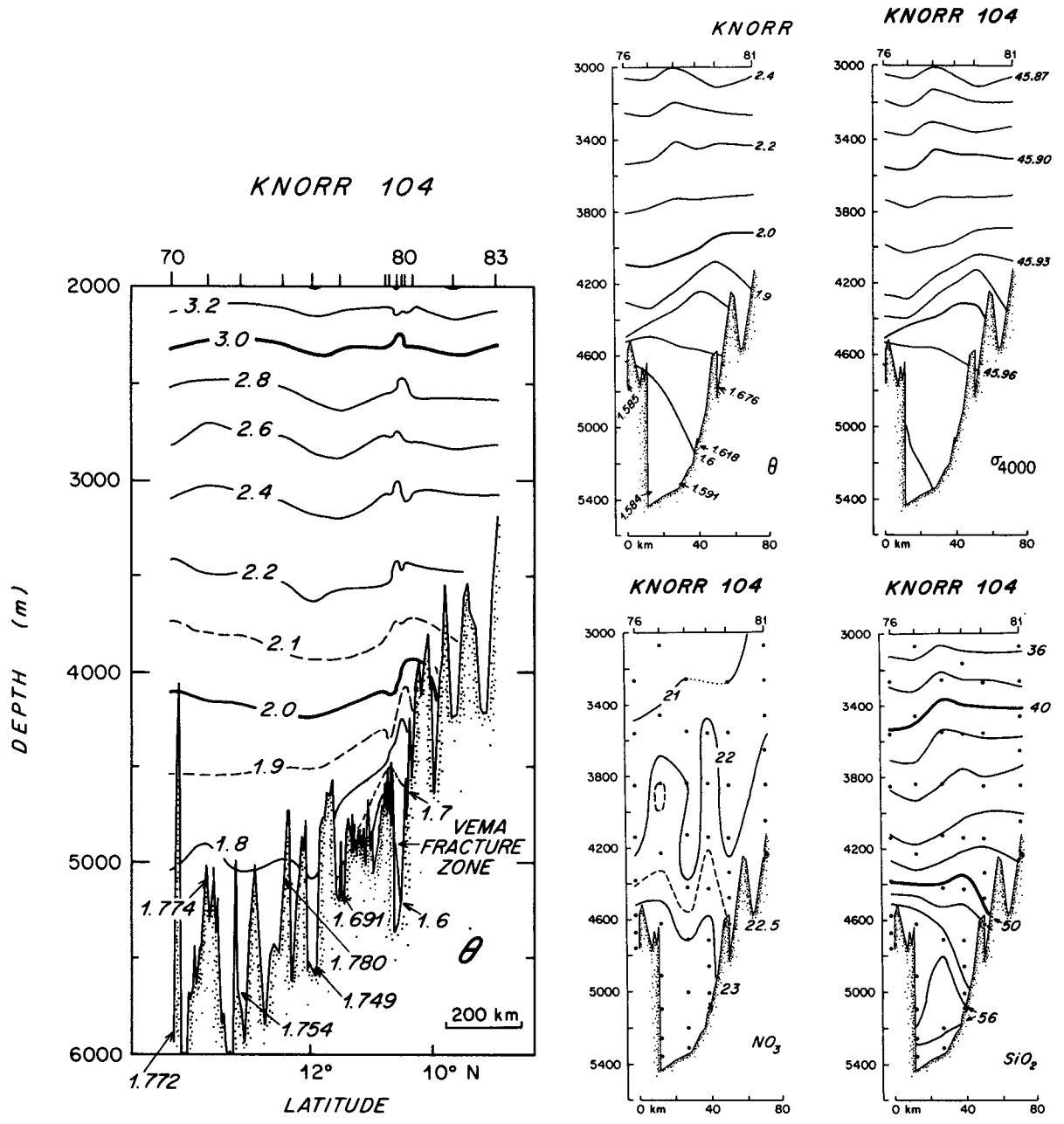

FIG. 8. The deep potential temperature distribution at the eastern exit of the Vema Fracture Zone (station locations Fig. 7a).

ways connecting the Vema deep to the eastern trough deeps. We have included near-bottom temperature values in the sill region. There seems no ambiguity in contouring a continuous pathway exceeding 4700 m. It is tempting also to contour a continuous pathway exceeding 4800 m, but this is precluded by the quasi-zonal trackline explicitly illustrated in Fig. 7b: its two observations of 4768 m near 39°W are the controlling depths, and thus are our best estimate of the sill depth within the overall resolution of the data.

A summary description of the topography of Fig. 7c is as follows. The Gambia Abyssal Plain of the eastern trough extends westward into this region at three locations: 10°40′, 11°15′ and 12°N. All three of these are zonally trending linear fractures included in the Heezen et al. description of the Vema Fracture region. The Vema enters this region from the west near 10°45′W trending just south of eastwards. There are two salient aspects of the Vema structure in this region between 40° and 38°W. First, the north wall deepens east of 39°W, giving a pathway exceeding 4700 m along which the Bottom Water that enters the region in the

Vema from the west can escape the Vema into (most directly) the southern pair of westward extensions of the Gambia Abyssal Plain. This pathway appears to have a sill depth near 4770 m. Second, the floor of the Vema has a major disruption east of 38°40'W. West of there, six tracklines well define the continuity of the floor exceeding 5000 meters. East of 38°15'W such depths again are found at about the same latitude, and these have been contoured elsewhere as extending far eastward (Heezen et al. 1964; Krauss 1964; Egloff 1972; Searle et al. 1982). But between 38°15'W and 38°40'W there is no indication of a deep corresponding to the Vema. The sill we have described then is a control sill for the total flow of water in the Vema, not just for a leak of some of that flow across the north wall. Below we will estimate the total flow in the Vema at 39°W. This total flow is required to flow into the Gambia Abyssal Plain along the silled passage just described, because there is no eastward continuation of the Vema across 38°30'W due to the major disruption of the floor at that longitude.

2) Downstream warming of bottom water

In Fig. 5 bottom temperatures are very uniform west of the primary sill and east of the exit sill. The essence of the highly successful Heezen et al. sill inference is the first-order approximation that the sill blocks the water colder than that found upstream of the sill at the depth corresponding to the sill. This actually is dynamically implausible, for it implies motionless fluid below sill depth and moving water above, which would require shear, which in turn would require a geostrophic signature of sloped isotherms at the level of the sill depth. Vangriesheim and Eittreim et al. show temperature profiles at 11 stations upstream of the primary sill. These show that the low gradient Bottom Water extends upward well above the sill depth. Since vertical shear requires a vertical density gradient as well as the horizontal isotherm slope, the weak vertical gradient in the Bottom Water precludes significant vertical shear across that layer. These authors do show strong vertical gradients between 4400 and 3700 m in the transition layer between the Bottom Water and the Deep Water, roughly 1.5° to 2.0°C. If this layer slopes across the Vema, then significant shear would result. Eittreim et al. do show two station groups aligned roughly cross the Vema at 44° and 43°35'W. Calibration problems preclude their use for geostrophic computations, but they do show that the layer slopes downwards to the north, the same as our section farther east (Fig. 8). This is the geostrophic signature of bottom-intensified eastward flow (relative to a mid-depth reference level), not of eastward flow in the transition layer decreasing towards the Bottom Water layer (which requires the opposite slope). We conclude then that some of the cold Bottom Water west of the sill flows up and over the sill.

If indeed the cold Bottom Water west of the sill flows up and over the sill, then why are the observed bottom temperatures at and immediately east of the sill warmer (Fig. 5)? Vertical mixing is the likely reason, and its signature is hinted at in the Vangriesheim CTD profiles. Her stations 2 and 3 near the sill, while having the same three layer overall structure as stations west of the sill, show two differences besides the warmer bottom temperature. First, the Bottom Water layer develops steppiness over the sill and second, the transition layer exhibits a sharp gradient—a jump of more than 0.1°C—near its top (1.9° to 2.0°C). Her station 195 km east of the sill shows a thick Bottom Water layer just warmer than 1.50°C, with very weak gradients extending over 700 m, and an increased vertical gradient over the next 300 m, culminated by a sharp increase from 1.6 to 1.8°C. Such jumps occur as the product of mechanical mixing homogenizing a layer in a stratified fluid. We believed that the warming trend illustrated in Fig. 5 reflects the turbulent overturning and mixing of the Bottom Water as it cascades down the east side of the sill and continues eastward along the Vema. By 200 km downstream of the sill, our *Knorr* section across the Vema (Fig. 8) shows the mixing having warmed the thick Bottom Water layer to about 1.58°C. These stations also show the jump at the top of the Bottom Water layer at temperatures between 1.65° and 1.95°C.

A similar process presumably occurs in the flow over the exit sill. The section just upstream of the sill (Fig. 8) shows substantial transport (discussed in the next subsection) of Bottom Water deeper than the sill depth and colder than that observed downstream of the sill. The piling up of the coldest water on the north side of the Vema against the sill, and the presence at station 76 of a thin layer (250 m) of this cold water atop the north wall, demonstrates the exiting of Bottom Water up and over the sill. Our *Oceanus* station 26 downstream of the sill has a steppy profile in the Bottom Water layer, capped by a sharp jump in temperature near 1.9°C.

3) Transport at the Vema exit sill

It will be argued in this section that the cold ($\theta < 2.0$°C) water transport exiting from the Vema is most likely between 2.08 and 2.24×10^6 m^3 s^{-1}, based on geostrophic calculations with reference levels between 2.17° and 2.49°C. These transport values are of clear significance to both eastern and western trough abyssal circulations, representing a bleeding-off of about a third or more of the estimated Bottom Water ($\theta < 1.9$°C) supply to the western tropical Atlantic, which is estimated as 2.3 to 2.8 ($\times 10^6$ m^3 s^{-1}) at 16°S to 8°N (Wright 1970) and 3.5 to 4.5 ($\times 10^6$ m^3 s^{-1}) at 13°N (McCartney and Speer, 1991).

Water mass characteristics are an aid to constraining

flow directions. We define four layers to aid our deductions of reference levels:

1) Bottom Water: <2.0°C, net eastward flow demanded, and eastward flow of all sublayers most plausible, because there is no source of cold water to the east, and because coldest temperatures increase west to east (Fig. 8).

2) Transitional Layer: 2.0° to 2.3°C water, net eastward flow most plausible because net eastward flow is demanded in bracketing layers 1 and 3 and water mass evidence for westward layer 2 flow is lacking.

3) Deep Water: 2.3° to 4.5°C water, net eastward flow demanded and eastward flow of all sublayers most plausible because the associated nitrate minimum must come from western trough.

4) Intermediate Water: 4.5° to 9.0°C water, net westward flow demanded and westward flow of all sublayers most plausible, because the associated nitrate maximum must come from near Africa.

Net flow means are summed over the layer temperature range and over all stations. We will refer to the sublayers within a given layer as "strata."

The Deep and Intermediate Water layers are defined and their flow directions constrained by the nitrate field

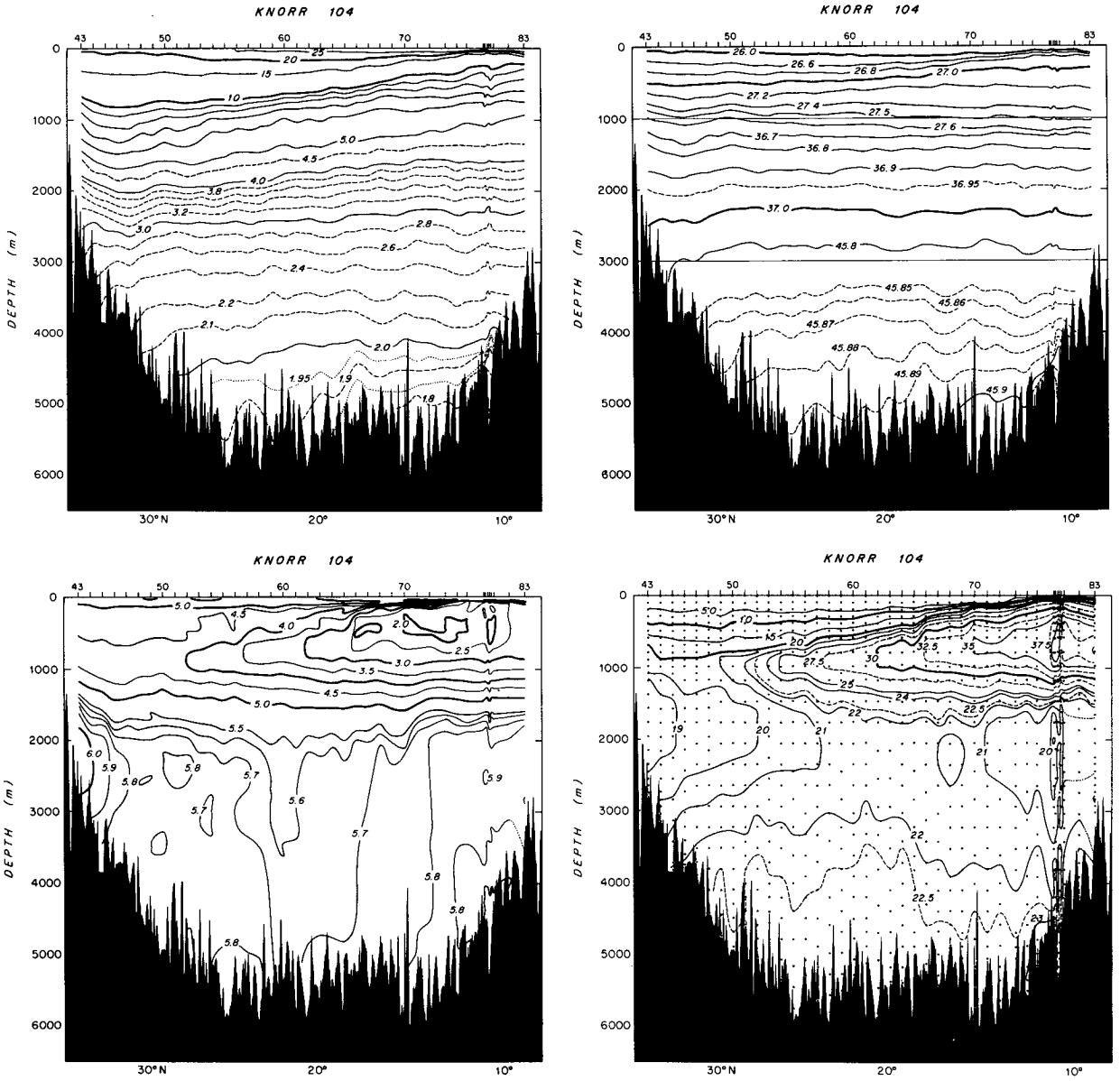

FIG. 9. Property distribution along the 1983 *Knorr* quasi-meridional section near 35°W (Fig. 3). (a) Potential temperature (°C). (b) Density parameters σ_0, σ_2, and σ_4 (g kg^{-1}). (c) Dissolved oxygen (ml l^{-1}). (d) Nitrate (μmol l^{-1}).

(Fig. 9d). Two laterally isolated vertical nitrate extrema are seen at the Vema stations. The colder extremum, a minimum with values falling below 20 μmol l^{-1}, extends from $\theta = 2.6°$ to 3.9°C (1600 to 2800 m). This is western basin Deep Water, and its isolated position in the section, surrounded by higher nitrate eastern basin waters, requires that it flow eastward from the western trough. The second extremum, a maximum with values exceeding 40 μmol l^{-1}, extends from $\theta = 5.5°$ to 9°C (400 to 900 m). This seems to be a form of Antarctic Intermediate Water (broadly speaking) that has nitrates exceeding 37 μmol l^{-1} and is found in the eastern trough off western Africa. In the *Knorr* 35°W section, it is found only within the Vema. There is no western source of such high nitrate, and thus it must be flowing westward from the eastern trough.

The potential temperature/nitrate relationships for the Vema station group and for the nearest station group to its north are shown as mean curves and standard deviation envelopes (Fig. 10). The standard deviation envelopes are distinct for two potential temperature ranges: 2.3° to 4.2°C, part of our Deep Water layer, and 4.7° to 9.0°C, part of our Intermediate layer. For simplicity, the intervening 4.2° to 4.7°C layer is split at 4.5°C and added to the Deep and Intermediate Water ranges. In what we have defined as the Transitional Layer (2.0 to 2.3°), the nitrate characteristics are not distinct, and thus do not constrain the flow direction.

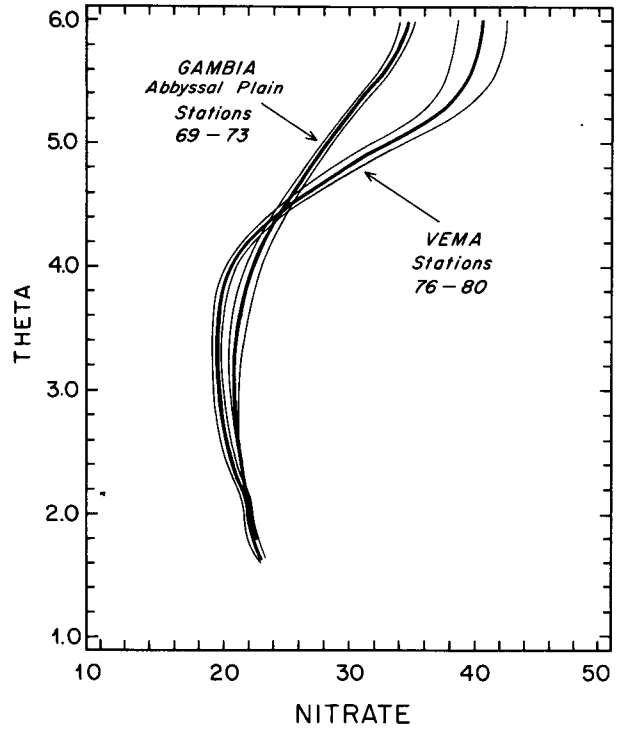

FIG. 10. Average nitrate–potential temperature relation and standard deviation envelopes for two station groups from the 1983 *Knorr* section near 35°W (Fig. 9). Stations 76–80 fall in the Vema Fracture Zone, stations 69–73 immediately to the north in the Gambia Abyssal Plain.

The deep vertical shear field (proportional to isopycnal slope times the vertical density gradient) is dominated by isotherms in the upper part of the Bottom Water layer rising about 400 m to the south, indicative of eastward flow relative to a shallower reference level. The vertical temperature gradient and thus vertical shear are greatest near $\theta = 1.9°$C. The reversed slope of the 1.6°C isotherm contributes little reversed shear because the vertical density gradient at that level is small. More significant shear reversals are found above the Bottom Water layer, giving an "S" shape to the velocity profile in the Deep Water. For a range of reference levels (see below) it is possible (though arguably implausible) for parts of the Transitional Layer and Deep Water Layer to flow westward, vertically sandwiched between eastward flowing Bottom Water and Deep Water.

Given the observed shear field, transports in each layer hinge on the choice of reference level (which will be taken as a level of no motion). The flow direction constraints are derived from the water mass characteristics, and are best dealt with as functions of temperature rather than depth. Thus, isothermal reference levels are considered rather than isobaric; Fig. 11 shows the dependence of the four layers' net transports on the reference level temperature. Vertical lines numbered I through V indicate a succession of reference level limits developed in the next few paragraphs.

As the reference level is raised from the bottom into the Bottom Water, the Bottom Water flow initially is the wrong way, westward, because most of the shear in the layer is above the reference level. The net Bottom Water transport turns eastward for reference levels warmer than 1.83°C, but the warmer strata of the Bottom Water continue to have westward transport until the reference level reaches 1.86°C. This (line I, Fig. 11) is the initial lower bound on the reference level, which in turn gives an initial lower bound on the net Bottom Water transport of 0.46×10^6 m^3 s^{-1}.

The next constraint we consider is the requirement of net westward flow of the Intermediate Water. Reference levels warmer than 4.79°C give net eastward transport in this layer—not allowed. Requiring the individual strata with distinctly elevated nitrate (warmer than 4.7°C, Fig. 10) to flow east reduces this upper reference level limit to 4.7°C, with a corresponding Bottom Water transport of 3.48×10^6 m^3 s^{-1}. Requiring all the individual strata of the Intermediate Water to move west, that is, all the water warmer than 4.5°C, reduces the upper reference level limit a bit more, to 4.5°C (line II, Fig. 11), with the corresponding Bottom Water transport of 3.05×10^6 m^3 s^{-1}. This last step seems shaky at this point, as there is no water mass contrast near 4.5°C to justify it (Fig. 10), but other evidence supports it, as discussed next.

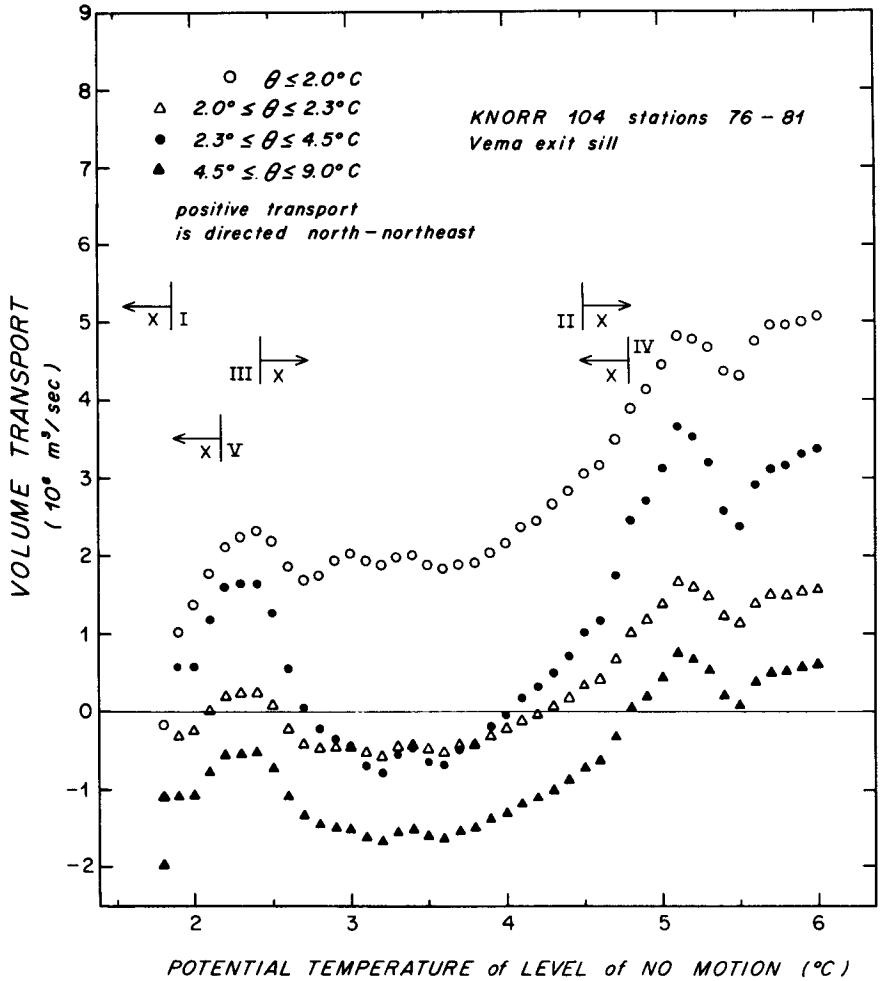

FIG. 11. Transport of water as a function of the assumed potential temperature of an isothermal "level" of no motion. *Knorr*-104 section at the Vema Fracture Zone exit sill (Fig. 8).

Application of the Bottom Water and Intermediate Water constraints has limited the range of reference levels to 1.86° to 4.5°C (between lines I and II in Fig. 11). For this allowed range of reference levels, the Bottom Water transport is bracketed between 0.46×10^6 m^3 s^{-1} and 3.05×10^6 m^3 s^{-1}. These ranges can be further limited by considering the constraints indicated by the Deep Water and the Transitional Layer. We require the net transport of the Deep Water to be eastward, and this excludes the reference level range 2.72° to 4.02°C. This excluded range is enlarged based on two plausible grounds (that independently give essentially the same reference level range). One is that the transitional layer also moves eastward; the other is that all the strata of the Deep Water move eastward together. These broaden the excluded range (lines III and IV in Fig. 11) to 2.43° to 4.80°C. Note that line IV lies warmer than line II in Fig. 11. What this means is that all the warmer reference levels have been excluded because they give either low nitrate water of western origin flowing westward in some Deep Water strata (this constraint centers at a velocity extrema at 2.4° to 2.45°C) or high nitrate water of eastern origin flowing east in some Intermediate Water strata.

The allowed reference level range has been closed to 1.86° to 2.49°C (between lines I and III in Fig. 11). The final range narrowing also reflects the Deep and Intermediate Water's constraints. Requiring all individual strata of the Deep Water to flow eastward as well as the layer net raises the lower bound of the reference level to 2.17°C (line V in Fig. 11). The allowed range 2.17° to 2.43°C (lines V and II in Fig. 11) corresponds to a range of net transport for the Bottom Water of 2.05 to 2.32 ($\times 10^6$ m^3 s^{-1}). Accompanying this Bottom Water flow is a combined transitional layer and Deep Water eastward transport between 1.4 and 1.9 ($\times 10^6$ m^3 s^{-1}), overlain by a westward transport of about 0.6×10^6 m^3 s^{-1} of Intermediate Water. These narrow ranges are the result of requiring eastward transport in all the individual strata of the lower three

layers in addition to the three layers' required net eastward transport, and requiring westward flow in all the Intermediate Water strata as well as that layer's net westward transport.

At other locations there is evidence that a reference level in the transitional layer or lower Deep Water is appropriate. In general, Bottom Water transport estimates will be given using a range of reference levels between 2.0° and 2.5°C. In subsequent figures we will give transport details for a broader range of reference levels, as in Fig. 11. Throughout, vertical shear beneath the deepest common level will be estimated from the observed isopycnal slope at that level and the vertical density gradient beneath that level at the deeper of the two stations. Sometimes adjustments to the cold water transport will be made reflecting the possible disruption of the geostrophic balance by abyssal bathymetry between two stations.

4) 1983 TRANSPORT COMPARED TO EARLIER ESTIMATES

Both Vangriesheim (1980) and Eittreim et al. (1983) estimated cold water transport in the Vema from the cold water cross-sectional area multiplied by the time-averaged down-channel velocity component from short-duration near-bottom current meter records. The resulting transport estimates for water colder than 1.5°C ranged from nearly zero to 0.46×10^6 m^3 s^{-1}. All of Vengriesheim's and Eittreim et al.'s current meters were deployed on the flanks of the Vema or on the sill itself; instrument pressure limitations precluded placing instruments in the central channel. Deployment durations were short, between 1 and 33 days. Neither Vangriesheim nor Eittreim et al. have data suitable for geostrophic calculations, though the latter paper includes a temperature section at 42°35'W showing sloping isotherms suggestive of eastward geostrophic flow.

Our transport range lower bound (2.08×10^6 m^3 s^{-1} for water colder than 2.0°C) is nearly four times the largest Vangriesheim estimate (0.46×10^6 m^3 s^{-1} for water colder than 1.5°C). Can these be reconciled? The answer seems to be yes: the channel area occupied by water colder than 1.6°C is 19% of the area occupied by <2.0°C water and velocities are bottom-intensified, bringing the <1.6°C transport proportion to 25 or 30%, in line with the ratio between Vangriesheim's and our observed transports. Bottom speeds at our *Knorr* section (Fig. 8) are about 20 cm s^{-1} for reference levels in the preferred range; Vangriesheim's current meter velocity near the bottom was 33 cm s^{-1}.

Another estimate, of 0.0 to 0.7×10^6 m^3 s^{-1} eastward transport through the Vema, was produced by the box model inversion of Schlitzer (1987) using physical and chemical tracers. It appears that these low values, compared to our observations, resulted from an inaccurate representation of Vema inflow characteristics, in particular an excessively low δ^{14}C value. Additionally, his estimate is for an *average* Vema temperature of 1.5°C, and hence would have to be adjusted for the volumetric dilution required to raise that to the observed value.

The model flows are quite sensitive to the ^{14}C balance. As Schlitzer (page 2962) says, the Vema flow upper bound is constrained by ". . . the ^{14}C balance of the box into which the [Vema] inflow is directed." Also, the model's eastern Atlantic δ^{14}C balance drives equatorial downwelling: this peculiar circulation is required ". . . because of the low δ^{14}C content of the west Atlantic water flowing through the Romanche and Vema fracture zones into the east Atlantic." With this equatorial downwelling system, the model requires Bottom Water transport of 2.6 to 5.1 ($\times 10^6$ m^3 s^{-1}) flowing eastward through the Romanche and 2.5 to 5.0 ($\times 10^6$ m^3 s^{-1}) flowing northward through Kane Gap.

Schlitzer uses a value of −122‰ for the Vema inflow, lower than that in all model boxes except the equatorial deep water box; values between −117 and −119‰ are used for the Cape Verde and Canary basin boxes. A better δ^{14}C value for the Vema Bottom Water inflow would be in the range −115 to −110‰, that is, *higher* than the boxes it flows into rather than *lower,* judging from two pairs of δ^{14}C observations. One pair (−125‰ at 1.18°C and −104‰ at 1.76°C) comes from GEOSECS station 37 (12°N, 51°W) in the Vema's western trough source region; the station has oxygen and nutrient profiles similar to stations in the Vema (Bainbridge 1981; Östlund et al. 1987). The second pair (−105.6 at 1.86°C and −119.5 at 1.36°C) comes from TAS station 20 (Östlund and Grall 1987), located less than 20 km south of our 13°N western basin transect station 15 (Fig. 6). Interpolating linearly to the Vema primary sill temperature (1.40°C) gives δ^{14}C values of −117‰ and −118.5‰ at the GEOSECS and TAS stations, respectively—both significantly higher than Schlitzer's value. And these provide in effect a lower bound: Vema Bottom Water inflow mean temperature must be higher than the sill temperature, and thus a mean δ^{14}C value of −115 to −110‰ is likely.

We predict rather different model Romanche, Kane Gap, Vema, and upwelling flows, if the Vema δ^{14}C value is changed to a more realistic value. The other Vema inflow characteristics (average temperature, silica, etc.) also need to be adjusted.

5) RELATIONSHIP WITH THE WESTERN TROUGH TRANSPOSED BOTTOM WATER CURRENT

A well-known curiosity of the abyss of the North Atlantic eastern trough is its "transposed" Bottom Water current (Warren 1981; Wright 1970; McCartney and Speer 1991), so-called because it is found on the eastern side of the western trough. Its geostrophic signature, an eastward 500 m rise in the depth of isotherms near 2.0°C (Fig. 6), means that the water at the sill

depth of the Vema is colder than it would be if the Bottom Water were not transposed. Temperatures at low-latitude stations along the western flank of the ridge (e.g., station 18, Fig. 6) have temperatures of 1.45°C at the depth of the Vema primary sill, while stations farther west have temperatures of 1.73°C (station 11, Fig. 6).

As a result, it is tempting to say that the existence of a transposed distribution of Bottom Water in the western trough is responsible for the magnitude of eastward transport of water colder than 2.0°C through the Vema. But could it be the other way around? Does the Vema eastward leak (which supplies deep water for eastern trough upwelling) in some way help to cause the western trough Bottom Water to bank eastward up against the ridge western flank? This question is explored in a companion study (Speer and McCartney 1991).

3. The influence of Vema waters on the eastern trough

a. Eastern trough Bottom Water sources

Eastern trough bottom water is derived from flow through the Vema Fracture Zone into the Gambia Abyssal Plain and from flow through the Romanche Fracture Zone into the Sierra Leone Basin. We argue below that the Vema influence determines the abyssal water mass characteristics of the northeastern Atlantic basins north of the Sierra Leone Rise (the Gambia Abyssal Plain, the South Canary Basin, and the North Canary Basin), and that the influence of Romanche waters on these basins is slight.

Northward flow of the coldest Romanche waters into the Gambia Abyssal Plain is obstructed by the Sierra Leone Rise. The deepest passage through the rise is Kane Gap. The gap's sill depth is between 4389 and 4572 m (Hobart et al. 1975; Egloff 1972; their charts' 2400 and 2500 uncorrected fathom contours), separated along-channel by a deep of about 4700 m. There is a second, longer and shallower passage through the rise, west of the gap, that consists of a broad region shallower than 4500 m silled at about 4300 m (Fig. 1, and Searle et al. 1982).

Hobart et al. (1975) were the first to suggest that deep eastward and northward flow from the Vema might predominate overflow through the gap in determining the characteristics of the plain abyss. They based this idea on the eastward warming observed in two thermoprobe measurements in the plain well west of the gap (θ_B = 1.829°C at 22°W and 4815 m, and θ_B = 1.799°C at 25°W and 5641 m). Indeed, Hobart et al. wondered if flow through Kane Gap might be southward, noting that sediments there had been disturbed by flow, but they were not able to deduce the flow direction (although a bottom photo showed sediments streaming north).

The Kane Gap sill temperature is about 1.89°C (estimating from the temperature at the approximate sill depth, 4500 m, on a station just to its south, Tropical Atlantic Study station 99, Scripps Institution of Oceanography 1986). Bottom temperature observations in the gap deep channel are 1.851°C at 4707 m, 1.854°C at 4673 m (at two additional Hobart et al. thermoprobe measurements, accuracy quoted as 0.01°C), and 1.867°C at 4660 m on the TAS station mentioned above.

Thus, Kane Gap sill water (1.89°C) is much warmer than Vema sill water (1.40°): indeed, a 1100 m thick layer of water colder than gap sill water was found well north of the Vema (*Knorr* station 72, Fig. 8) with a bottom temperature of 1.754°C. A similar layer 1200 m thick was found about halfway between the gap and the Vema (*Oceanus* station 100, Fig. 12a), with θ_B = 1.772°C at 5704 m.

b. Lateral extent of Vema influence

The extent of the Vema's influence on abyssal characteristics of the Gambia Abyssal Plain and the Canary Basin abyssal characteristics can be seen clearly in the near-bottom temperature field (Fig. 13). The data used to produce this detailed picture include Mantyla and Reid's (1983) carefully examined and edited data; the 1983 *Oceanus* and *Knorr* stations; the 1981 *Atlantis II* 24° and 36°N sections; a 1988 *Oceanus* section near 25°W plus five stations near 22°W (made by Tsuchiya et al. 1991); the few Tropical Atlantic Study stations that reach to <100 m above the bottom; the 1989 *Oceanus* 11°N section (kindly supplied by Dean Roemmich and Mindy Hall); the GEOSECS and TTO/TAS stations in the area; some *Meteor* and *Rambler* stations included in Wüst's original study (1933); and, lastly, some early *Crawford* stations that fill out the picture near the Sierra Leone Rise and Cape Verde Ridge. This data is not intended to be all-inclusive, just adequate for perceiving basin-scale trends. The isotherm contours are noisy because they are unsmoothed and contoured at a small contour interval (0.02°C), and because of real temperature variability introduced by small-scale topographic features.

Near-bottom temperatures in the Gambia Abyssal Plain generally increase eastward from the Vema to the gap, confirming Hobart et al.'s isolated thermoprobe observations. Just 300 km northwest of the Kane Gap sill (at our short 22°W section, Fig. 14) θ_B is 0.02° to 0.04°C colder than the gap sill temperature. The coldest temperatures (≤1.70°C) are observed at the Vema exit section (Fig. 8) and on the ridge flank north and east of the Vema (*Oceanus* station 26, Fig. 6; *Knorr* station 75, Fig. 8; and six of the 1989 11°N *Oceanus* stations, Fig. 5). The eastward spread through the Gambia Abyssal Plain of Vema cold water is shown to be strikingly narrow and zonal by the 1.70° to 1.76°C contours. The next heavy contour (θ = 1.80°C) encompasses a large area of the western and central Gambia Abyssal Plain, bounded in the south, north,

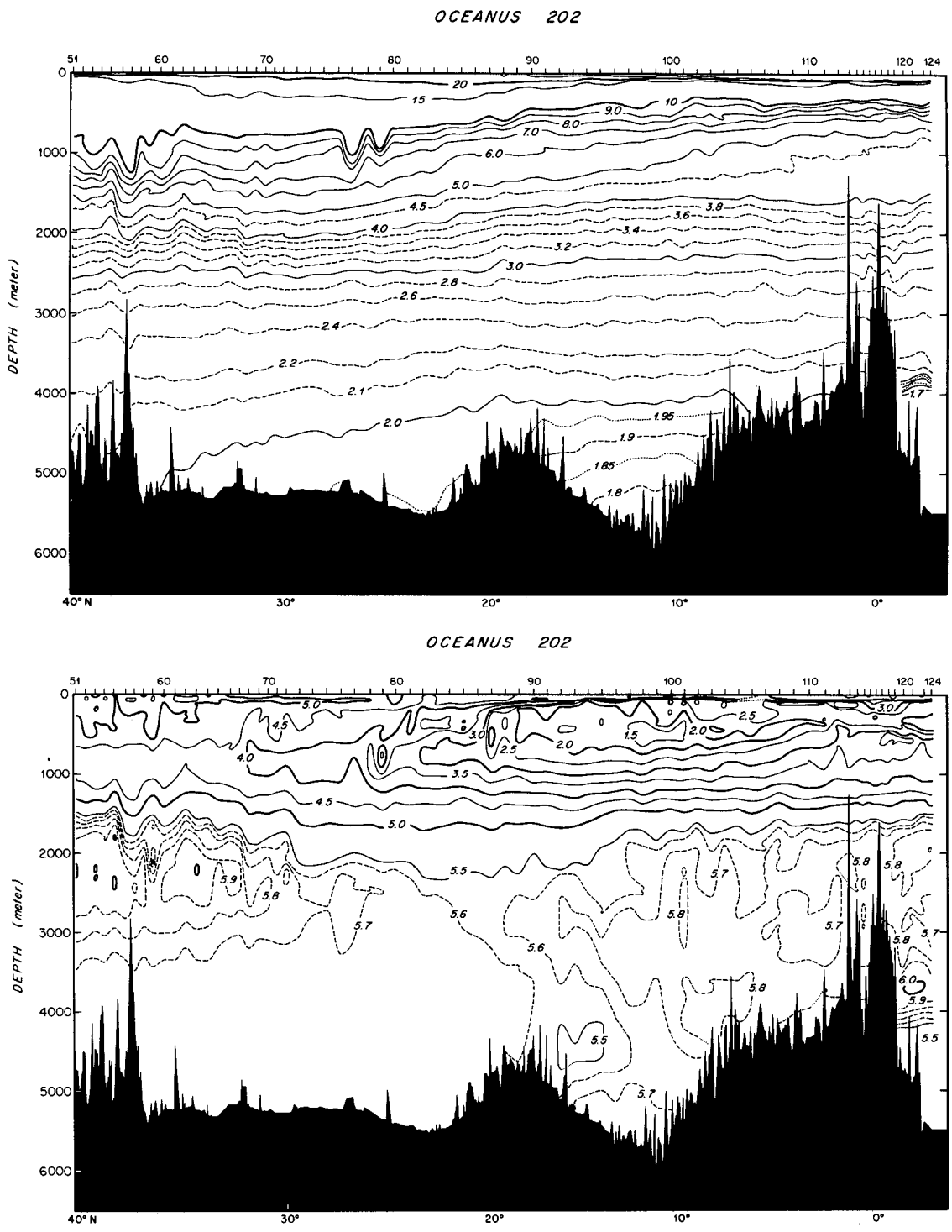

FIG. 12. Property distributions along the 1988 *Oceanus* quasi-meridional section near 25°–29°W (Fig. 3). (a) Potential temperature (°C). (b) Dissolved oxygen (ml l^{-1}).

and east, respectively, by the Sierra Leone Rise, the Cape Verde Ridge, and the shoaling depths towards Kane Gap.

Northward western-intensified flow in the northern Gambia Abyssal Plain and in the South Canary Basin is also evident in the crowded band of isotherms that

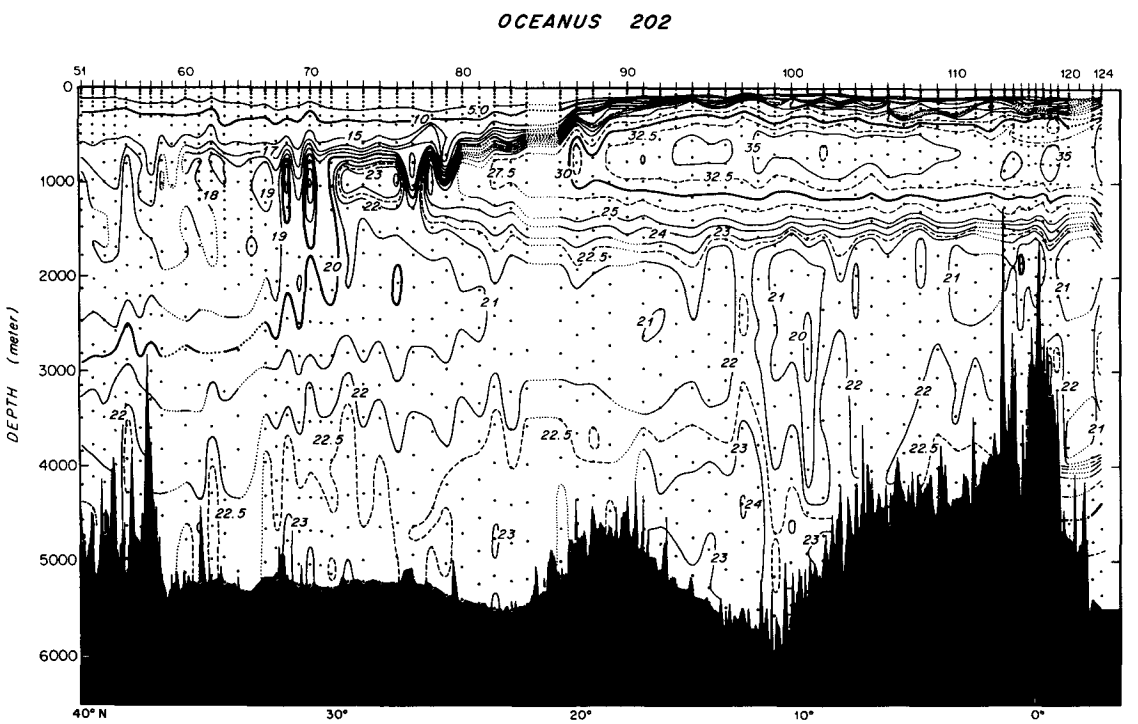

FIG. 12. (*Continued*) (c) Nitrate (μmol l^{-1}).

follows the Mid-Atlantic Ridge eastern flank northward from the Vema to at least 30°N. The coldest South Canary Basin observation (θ_B = 1.83°C) falls in its southwest corner, and is again colder than Kane Gap sill water.

c. *Abyssal circulation 1: Gambia Abyssal Plain*

Here and in section 3d below the abyssal circulation of the northeastern Atlantic basins is discussed. A circulation cartoon annotated with our favored transport estimates is given in Fig. 4. The explicit estimates are for a uniform reference level choice of 2.2°C. This falls in the middle of our constrained range at the Vema exit sill (Fig. 11 and section 2b), and also of the plausible range at other locations discussed below. The flow paths are highly schematic with widths of currents not shown. Curly tips to some flow lines reflect required upwelling across 2.0°C.

1) EASTWARD CURRENT IMMEDIATELY OUTSIDE THE VEMA

Abyssal flow exits the Vema over the exit sill. Our geostrophic calculations are for flow oriented roughly north-northeast (25° true). The Vema exit flow, shear, and topography (see section 2b) are adequately resolved by our high-resolution section (Fig. 6, *Knorr* stations 76 to 81).

After passing over the sill, the outflow from the Vema appears to turn eastward, as suggested by the region of nearly uniform bottom temperature in Fig. 5 (for distances greater than 300 km), and by the eastward oriented cold "tongue" in Fig. 13b. This flow must pass eastward through our primary *Knorr* section. We have a much less resolved image of this eastward current: just three stations at large spacing (Fig. 8, *Knorr* stations 74, 75, and 80) lying on a line that runs almost north–south, just northeast of the high-resolution Vema exit section. The dramatic northward descent of deep isotherms along this line (300 to 800 m, about twice the descent of isotherms across the Vema) indicates eastward flow relative to a shallower reference level, if the descent is attributed only to a geostrophic flow perpendicular to the section (100° true in orientation). A potential problem with this, that nothing can be done about, is that some part of the descent could reflect the turbulent overflow descending the flank of the Mid-Atlantic Ridge onto the Gambia Abyssal Plain, that is, isotherm descent following the flow rather than expressing the geostrophic balance across that flow. A second problem is the very rough bathymetry between our widely spaced stations (Fig. 7c). We have to indirectly estimate geostrophic pressure gradients for the "bottom triangle" (the water column beneath the deepest common level of a station pair) and to consider making allowance for intervening bathymetry rising into the bottom triangle or even above the deepest

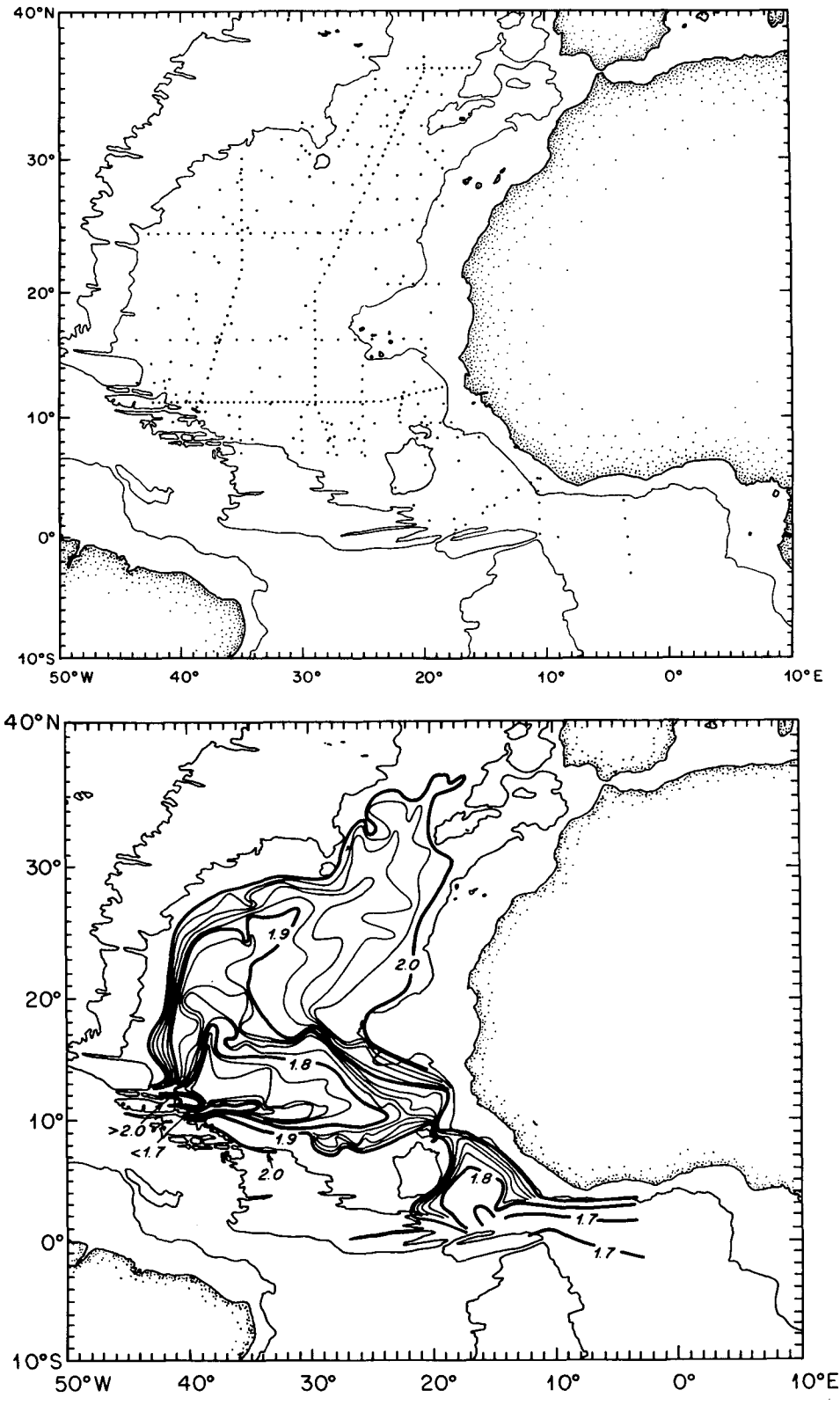

FIG. 13. (a) Location of the stations of the Mantyla and Reid (1983) database in the eastern trough merged with various recent data (see text) and Wüst (1933) stations. The IGY sections at 36° and 24°N (Fuglister 1960) have been deleted from the former database in favor of the Roemmich and Wunsch (1985) reoccupations in 1981. Only stations with data within 100 m of echosounding depth have been retained, with a very few exceptions where data farther up in water column documented a larger extension of a given isotherm (i.e., the water below will be even colder). These stations are open circles. (b) Contours of near ($\leq$100 m) bottom potential temperature in the eastern trough for the stations located as in (a). Contour interval is 0.02°C, and contours warmer than 2.0°C are not included.

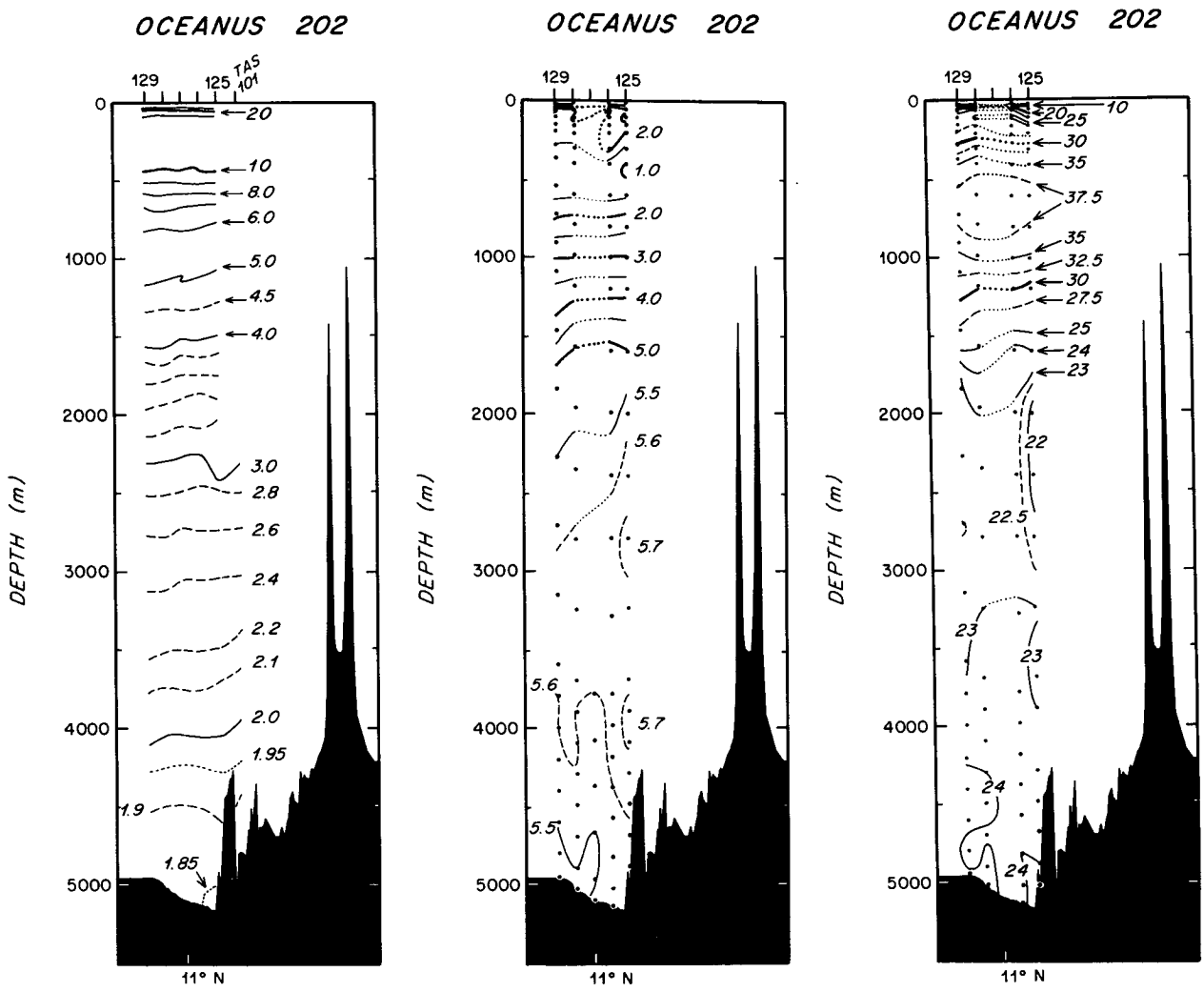

FIG. 14. Property distributions along the 1988 *Oceanus* quasi-meridional section segment near 22°W (Fig. 3). (a) Potential temperature (°C). (b) Potential density parameters σ_4 (g kg^{-1}). (c) Dissolved oxygen (ml l^{-1}). (d) Nitrate (μmol l^{-1}).

common level. Transport estimates for the eastward current are thus very uncertain. Geostrophic transport is in the range 1.3 to 3.0 ($\times 10^6$ m^3 s^{-1}) for reference levels in our favored range ($2.0° \leq \theta \leq 2.5°$C), including an adjustment for topographic blocking (Fig. 15). These values bracket the most likely Vema exit transport range [2.08 to 2.32 ($\times 10^6$ m^3 s^{-1}), section 2b]. On Fig. 4, the value 2.1×10^6 m^3 s^{-1} is plotted for the reference level 2.2°C.

Transport is significantly larger [5.1 to 8.4 ($\times 10^6$ m^3 s^{-1})] if the blocking adjustment is omitted (Fig. 15). The unadjusted transport computation ignores the topography and uses a simple bottom triangle (defined by the deepest common level of a station pair and deeper station's maximum depth). Here blocking is adjusted for by computing transport only for water above (i.e., warmer than that found at the level of) the highest significant intervening topography. This level is 1.85°C at station pair 74–75 and 1.80°C at pair 75–80 (filled circles, Fig. 15). The shear beneath these levels is ignored, and the corresponding transport assumed zero.

The higher, unadjusted transport range may be wrong and reflect nothing more than the inability of our few widely spaced stations to resolve the shear with respect to the shorter scale topography (the section crosses three 30 km wide fractures parallel to the Vema, while station spacing is 70 and 102 km). They could also be wrong because of having to assume that the total isotherm descent reflects the geostrophic velocity and neglecting the fraction that could be an ageostrophic descent of isotherms following the flow. Alternatively, the larger transports could be real and reflect augmentation of Vema exit transport from some

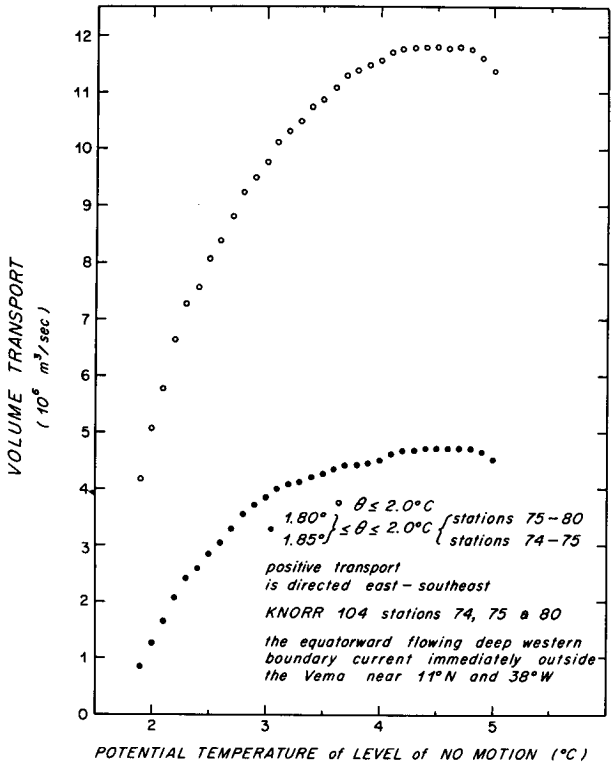

FIG. 15. Transport of water as a function of the assumed potential temperature of an isothermal "level" of no motion. *Knorr*-104 section defining the east–southeast flow of the boundary current in the western Gambia Abyssal Plain (Fig. 8).

source. Three physical mechanisms come to mind: cold water flow through other fractures, entrainment of warmer water or recirculation.

We cannot rule out the first of these alternatives. Sill depths are not well known for the nearby parallel fractures initially described by Heezen et al. (1964). The Searle et al. (1982) contouring of this region (at 500 m contour interval) shows all sills between 4000 and 4500 m. But that same chart shows the Vema less than 5000 m between 40° and 38°W, in disagreement with Fig. 7c. In our *Oceanus* section across the Mid-Atlantic Ridge (Fig. 6) we passed just north of the axis of one of these, and did place station 20 in 4235 m in the rift valley extending northwards from the fracture and recorded a fairly cold bottom temperature of 1.89°C. This temperature could reflect the controlling sill depth in the adjacent fracture. The impact of this station is evident in our bottom temperature chart (Fig. 13b), but there is nothing in nearby data that is compelling as to any additional cold source. Indeed, stations along this fracture show a cooling trend from the rift valley eastward to our *Knorr* station 74 (Table 1) which could indicate a westward flow from the Vema outflow towards the rift.

Entrainment is another possibility for an increase in the eastward transport outside the Vema. The coldest water being transported is warmer, and the transport weighted average temperature is also. One way of achieving this is to entrain a mass flux of warmer water across the 2.0°C isotherm into the Bottom Water, which simultaneously would elevate the average temperature below 2.0°C and increase the mass transport.

A recirculating component of the kind mentioned by Warren (1981, see section 1, second quote) could also contribute: boundary current transport is determined by basinwide mass balance requirements driven by both pointlike sources such as the Vema and distributed upwelling (Stommel and Arons 1960). The limited spatial coverage of the data along the Mid-Atlantic Ridge flank precludes our exploring further these alternatives.

2) EASTWARD FLOW ALONG THE PLAIN'S SOUTHERN BOUNDARY

(i) *Mass and property fields at 29° W*

Some of the eastward current flow, we argue, feeds into flow along the southwestern and southern boundaries of the Gambia Abyssal Plain. This boundary flow can be seen as a cold ($\theta < 1.76$°C) water tongue extending eastward from the Vema (Fig. 13b). The Mid-Atlantic Ridge flank and the Sierra Leone Rise bound the plain south of the latitude of the Vema (Fig. 1): at 4500 m depth, the ridge flank is oriented east-southeastward, turning eastward 3° farther south, and meeting the eastward-oriented rise about 5° farther east. The cold tongue seems pressed up against this boundary.

The mass and property field signatures of the eastward flow along the rise flank are illustrated by the *Oceanus* "29°W" section (Fig. 12; this *Oceanus* data delineates the 1.78°C θ_B contour of Fig. 13b). In the temperature section (Fig. 12a), isotherms < 1.95°C descend northward from the rise flank (station 103) towards the Cape Verde Ridge, indicative of eastward flow relative to a shallower reference level. Cold water along the rise flank is younger than water farther north, judging from the northward decrease in oxygen and increase in nitrate (northern stations 89 to 99 vs southern stations 99 to 103).

Property extrema in the rise flank flow and in the Vema exit flow are similar:

TABLE 1. Potential temperatures along the 12°N fracture zone.

Cruise	Station	Longitude (°W)	Depth (m)	θ_B (°C)
Knorr 104	74	38.2	5477	1.749
TAS*	67	39.3	5408	1.757
Oceanus 113	23	41.3	5109	1.799
Oceanus 133	20	44.8	4237	1.890

* Tropical Atlantic Study (Scripps Institution of Oceanography 1986)

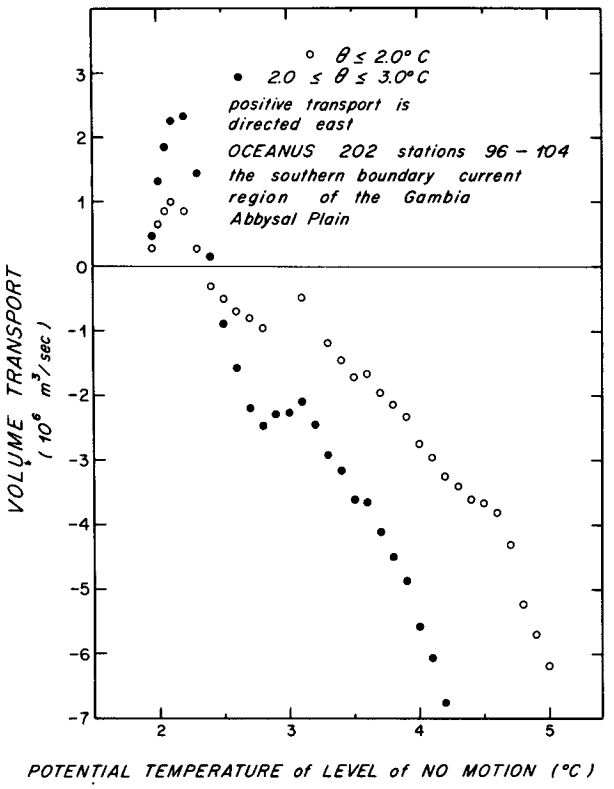

FIG. 16. Transport of water as a function of the assumed potential temperature of an isothermal "level" of no motion. *Oceanus*-202 section defining the eastward flow of the southern boundary current in the Gambia Abyssal Plain at midlongitude (Fig. 12).

(a) a slight oxygen minimum layer between the Bottom and Deep waters, defined at the Vema by the 5.8 ml l^{-1} contour (Fig. 9c) and at the rise flank by the 5.7 ml l^{-1} contour (Fig. 12b);

(b) a nitrate minimum layer in the Deep Water, defined at the Vema by the 20 μmol l^{-1} contour at 2.6 $< \theta <$ 3.9°C (Fig. 9d) and at the rise flank by the 21 μmol l^{-1} contour at similar temperatures (Fig. 12c, stations 99 to 102); and

(c) a nitrate maximum layer in the Intermediate Water, reaching values at the Vema of $\geq$37.5 μmol l^{-1} (Fig. 9d) and at the rise flank of 35.5 μmol l^{-1} (Fig. 12c, station 102, next to the strongest Deep Water nitrate minimum at station 101).

Both of the nitrate extrema were used to constrain the reference level choice at the Vema exit (section 2b). Paradoxically, the nitrate maximum core has higher values at 35°W (1983 *Knorr* data) than at 25°W (1988 *Oceanus* data), even though the core's source in the eastern trough off Africa is closer to 25°W. This may reflect interannual variability in the upwelling region farther east that is the source for this layer.

The maximum estimated Bottom Water transport of the rise flank flow is about 1.0×10^6 m^3 s^{-1}, computed from stations 96 to 104 using a reference level near 2.1°C. Transport dependence on reference level at the rise flank (Fig. 16) is different than at the earlier other locations (Figs. 11 and 15): the Bottom Water ($\theta < 2.0$°C) and lower Deep Water ($2.0 < \theta < 3.0$°C) move in the same direction (eastward for levels $1.9 \leq \theta \leq 2.35$°C) even when the reference level is between them, because isopycnal slopes reverse at about 2.2°C.

The rise flank cold water transport is significantly less than the transport of the eastward current just outside the Vema [1.3 to 3.0 ($\times 10^6$ m^3 s^{-1}); section 3c] where we do not have a very well-defined estimate and, more importantly, just inside the Vema where our well-constrained estimate [2.05 to 2.32 ($\times 10^6$ m^3 s^{-1})] is more than twice as large (section 2b). It is argued below (this section) that most of this decrease occurs where a northward deep western boundary current branches off the eastward current just outside the Vema.

(ii) *Flow dynamics*

The eastward flow in the southern Gambia Abyssal Plain could be interpreted as any one (or any combination) of three dynamical entities: (i) a topographically channeled jet, (ii) the southern boundary current of the Plain's abyssal circulation, or as (iii) a free jet supplying cold water from the Vema to the Kane Gap where it flows southward into the Sierra Leone Basin. We consider each of these possibilities in turn.

The first possibility is that the eastward flow is channeled by topography. The cold water tongue (Fig. 13b) extends eastward from the Vema exit along two fracture zones (Fig. 1) as they deepen eastward from 38°W to about 35°W, then follows the maximum depth pathway (>5500 m and sometimes >6000 m) east toward the Kane Gap, continuing toward it even as maximum depths decrease from 26°W to the gap. It appears that cold water trapping may occur only in the western part of this pathway: in the eastern part, at 29°W, the coldest temperature (θ_B = 1.764°C) at 29°W (Fig. 12a) does fall at the deepest station (station 99, 5959 m) but is not significantly colder than at an adjacent station (station 98, θ_B = 1.766°C at 5729 m), and only slightly colder (by <0.033°C) than at the other five deep stations at this longitude.

The second possibility is that the eastward flow is a southern boundary current that feeds the plain's interior abyssal circulation. A simple Stommel–Arons (1960) model for the eastern basin abyss consists of a rectangular basin with a mass source in the southwest corner and basin boundaries at the Mid-Atlantic Ridge to the west, Africa to the east, the Cape Verde Ridge to the north, and 10°N to the south. Given this geometry, plus upwelling through the thermocline and northward meridional velocity everywhere, the source flow bifurcates into (i) an eastward-flowing southern boundary current that supplies interior streamlines emerging from the (nonequatorial) southern boundary and (ii) a northward-flowing western boundary current

that supplies streamlines emerging from the western boundary. The observations are qualitatively well explained by the model, but the observed eastward extension of cold isotherms (Fig. 13b) seems more pronounced than such a model would predict.

The third possibility is that the eastward flow is, wholly or in part, a free jet that supplies Vema water to the Kane Gap where it flows southward into the Sierra Leone Basin. Southward flow at the gap can be represented in the model by a second, southeastern sink at or north of the southern boundary which causes a free eastward jet at the sink latitude. This jet would augment the southern boundary current. As it turns out, however, the observations, discussed in the next section, indicate that Kane Gap throughflow is negligible.

3) KANE GAP THROUGHFLOW

Traditionally, Bottom Water from the Romanche Fracture Zone has been thought to flow northward across the Sierra Leone Rise, through Kane Gap, into the northeastern Atlantic basins. We will now argue that the flow through Kane Gap is most likely negligible, neither significantly northward nor southward, based on geostrophic calculations in the plain and at the gap, and on a comparison of plain and gap water mass characteristics.

The Vema and Romanche fracture zones and their throughflows have rather similar characteristics (Table 2). The Romanche throughflow magnitude has not yet been determined directly, but water mass characteristics clearly indicate that it supplies Bottom Water to the eastern trough basins south of the Sierra Leone Rise (the Sierra Leone, Guinea, and Angola basins).

How much, if any, Romanche influence passes northward across the rise through Kane Gap (sill temperature 1.89°C; section 3a) into the Gambia Abyssal Plain? Apparently, cold ($1.89° < \theta < 2.0$°C) water transport through Kane Gap is essentially zero for reference levels colder than 2.7°C (Figs. 17 and 18). Shear is negligible in the lower Deep and Bottom waters at the gap, in contrast to all previously discussed shear and transport fields where significant cold water transport resulted from deep shear in the cold layers themselves. Water mass characteristics also seem to rule out northward flow: Bottom Water in the gap is more like the Bottom Water found in the plain than in the Sierra Leone Basin.

Negligible Kane Gap throughflow of water < 2.0°C is the only solution consistent with the Gambia Abyssal Plain transport field when the same isotherm reference level is used both at the gap and in the plain. The argument is as follows. Physically, the eastern plain is a cul-de-sac below the Kane Gap sill temperature (1.89°C). The *net* east–west cold water (<1.85°C) transport across 29°W goes to zero as required (Fig. 19) at a reference level of 2.2°C; while simultaneously, the eastward current transport reaches nearly a maximum (Fig. 16) at this same reference level. A reference

TABLE 2. Comparison of Vema and Romanche fracture zones.

Feature	Vema Fracture Zone	Romanche Fracture Zone
Entry sill	None (open to Demerara Abyssal Plain, 5190 m; Heezen et al. 1964)	4070 m (Metcalf et al. 1964)
Western trough θ at depth of entry sill	1.33°C (*Oceanus* 133-16)	0.68°C (*Oceanus* 202-124)
θ_B in zone west of main sill near Mid-Atlantic Ridge crest	1.30°–1.34°C (Various, see text)	0.68°C *Chain* 316 (Metcalf et al. 1964)
Main sill depth	4650 m (Vangriesheim 1980)	3750 m (4050 m)[a] (Metcalf et al. 1964)
Main sill θ_B	1.40°C (Vangriesheim 1980)	?? (1.29°C)[1] (*Chain* 315, lies southeast of sill, see Metcalf et al. 1964)
θ_B in zone east of main sill near Mid-Atlantic Ridge crest	1.58°C, 230 km east (*Knorr* 104-77)	1.52°C, 380 km east (*Chain* 302) (Metcalf et al. 1964)
Exit sill	≥4700 m	North into the Sierra Leone Basin: >4600 m South into the Guinea Basin: <5000 m
Coldest observed θ_B outside eastern zone in the nearby eastern trough	1.691°C (*Knorr* 104-75) in the western Gambia Basin	1.694°C (SAVE 35) in southern Sierra Leone Basin
	1.824°C (*Knorr* 104-66) in southwestern Cape Verde Basin	1.661°C (AJAX 8) in northern Guinea Basin

[a] At the Vema, Heezen et al. (1964) inferred the sill depth quite accurately by observing the bottom potential temperature east of the sill, and estimating the sill depth as the depth at which that temperature was found in profiles west of the sill. Metcalf et al. (1964) adopted a different approach at the Romanche Fracture Zone. They estimated the sill depth as the depth at which the depth profiles of temperature and salinity east and west of the sill diverged. It would seem that this gives the depth below which the basins are essentially isolated, but not the likely depth of the sill of the connecting pathway. They noted that the salinity and temperature profiles gave different estimates, 3925 and 3750 m, respectively. We can apply the Heezen et al. method to the Romanche Fracture Zone using the eastern and western basin temperature and salinity profiles in the Metcalf et al. paper. The coldest freshest observation they called eastern basin was observed at *Chain* station 302, which they noted may be isolated from the open eastern basin by another sill. Water of this temperature and salinity is found at about 4000–4100 m in the western basin, which is taken as a better estimate for the primary exit sill. Stations more clearly in the open eastern basin have slightly warmer and saltier Bottom Water ($\theta_B = 1.70$°C). These characteristics are found at 4600 m at station 302, which then is an estimate of the exit sill between the eastern Romanche Fracture Zone and the open eastern basin.

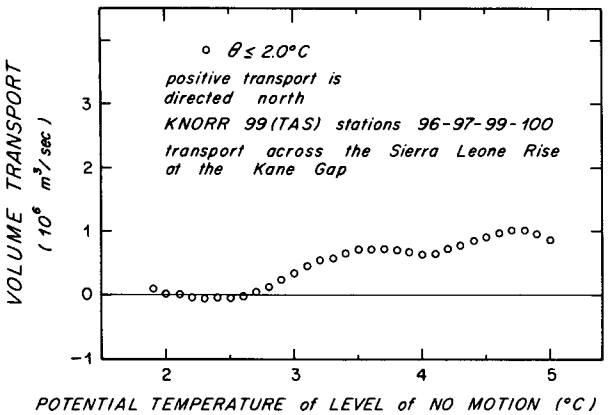

FIG. 17. Transport of water as a function of the assumed potential temperature of an isothermal "level" of no motion. *Knorr* Tropical Atlantic Study (Scripps Institution of Oceanography 1986) section near 9°N across the Kane Gap (station 98 not used for transport estimate due to low-quality data) (Fig. 18).

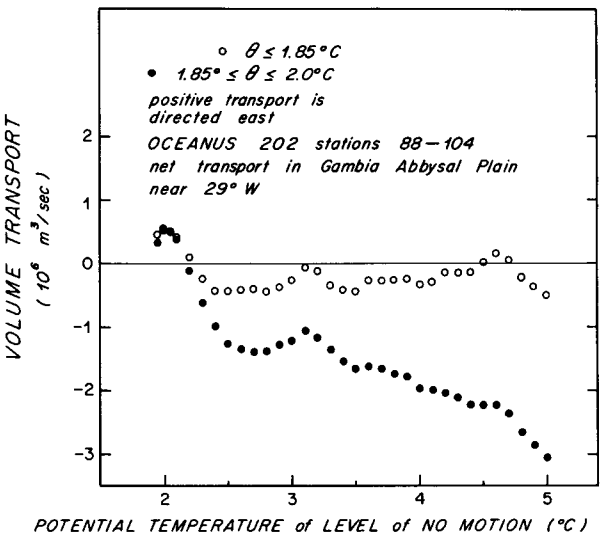

FIG. 19. Transport of water as a function of the assumed potential temperature of an isothermal "level" of no motion. *Oceanus* 202 section across eastern Gambia Abyssal Plain near 29°W enclosing a cul-de-sac for $\theta \leq 1.85$°C (Fig. 12). Transports are section net.

level colder than this generates net eastward cold flow across 29°W, which for mass balance demands intolerably large upwelling in the eastern plain (on the order of 17×10^{-5} cm s^{-1} for net east–west transport of 0.5×10^6 m^3 s^{-1}, given that the area bounded by 1.85°C isotherm west of 20°W is only 0.3×10^6 km^3). A reference level warmer than this produces a southern boundary current flowing unacceptably westward from warm to cold. This same reference level, the one giving no net transport colder than 1.85° across 29°W, simultaneously gives no net transport between 1.85° and 2.0°C at 29°W (Fig. 19), the part of the Bottom Water not blocked at the Kane Gap sill. This is gratifyingly consistent with the negligible Bottom Water transport at the Kane Gap (Fig. 17). The eastern Gambia Abyssal Plain is thus effectively a cul-de-sac for the total Bottom Water system, which seems to be a cyclonic gyre extending across 29°W.

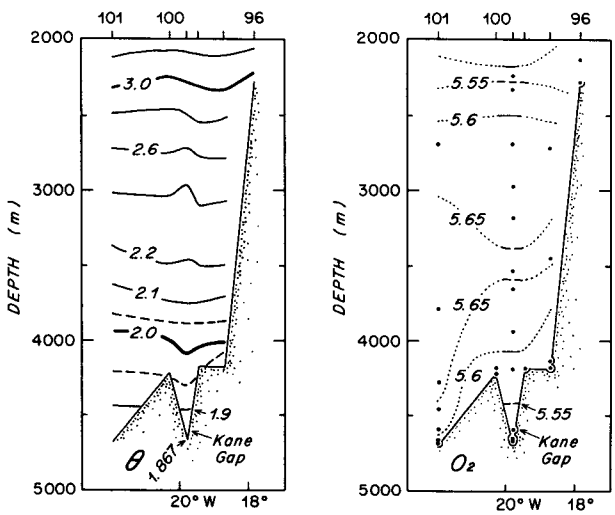

FIG. 18. Property distributions along the 1983 *Knorr* zonal section segment near 9°N (Fig. 3, and data from Scripps Institution of Oceanography 1986). (a) Potential temperature (°C). (b) Dissolved oxygen (ml l^{-1}). Only station 99 has data adequate for oxygen contouring.

4) CYCLONIC GYRE IN THE EASTERN PLAIN

Additional support for and details of this image of a cyclonic gyre in the eastern plain is given by the tracer fields. A relatively direct return path for the coldest part of the eastward current (<1.85°C) is indicated by the fact that at 29°W the return flow's near-bottom oxygen and nitrate values differ little from those of the eastward flow to the south; proceeding through the gyre, oxygen and nitrate change by only −0.05 ml l^{-1} and +0.2 μmol l^{-1}. Indeed, the cyclonic gyre colder than 1.85°C barely reaches 22°W (Fig. 14).

The tracer fields suggest that the warmer Bottom Water ($1.85 \leq \theta \leq 2.0$°C) takes a longer path through a gyre that extends farther eastward (Fig. 4). Whereas for the coldest Bottom Water little tracer contrast between the eastward and westward flows was found at 29°W, substantial changes (about −0.3 l l^{-1} and +1.0 μmol l^{-1} for oxygen and nitrate, respectively) are found following the warmer Bottom Water, associated with the formation in the westward flow of a curious oxygen minimum (<5.5 ml l^{-1})/nitrate maximum (>23 μmol l^{-1}) layer centered at about 1.95°C. Related tracer signals can be seen at 22°W (Fig. 14). Unfortunately the

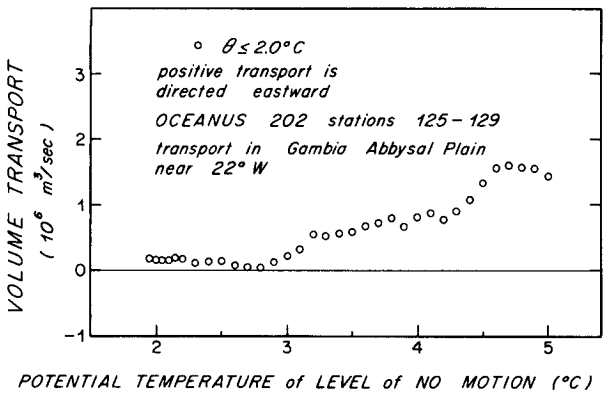

FIG. 20. Transport of water as a function of the assumed potential temperature of an isothermal "level" of no motion. *Oceanus* 202 section in eastern Gambia Abyssal Plain near 22°W (Fig. 14).

net transport of the warmer Bottom Water at 22°W cannot be computed as the section does not span the basin at the 2.0°C level. The short section appears to center on the midpoint of the gyre. A small eastward transport is calculated for our preferred reference level range (Fig. 20). The property section (Fig. 14) shows ample room to the north and south for the southern boundary current and the return flow to pass to either side of the section. Slight southward rising of the relevant isotherms at this longitude appears only when an adjacent station from the Kane Gap section is appended to the 22°W section.

These tracer changes could be partially explained by a longer path length for the warmer layer through a gyre extending farther eastward. The residence time of the warmer layer may also be longer, given the larger volume of this layer and the eastward current's transport as a function of temperature. Finally, the eastern plain continental rise, as described by Egloff (1972), is covered by "thick wedge of sediments" that "appears to be receiving biogenic pelagic sediment," possibly from the upwelling regime off West Africa. Contact with this layer could be causing elevated oxygen consumption and nitrate production; a low oxygen feature at 11°S beneath the Congo River plume was attributed to contact wth river-derived organic sediment on the continental rise (Warren and Speer 1991).

Whatever the cause of the low oxygen/high nutrient character of the warmer Bottom Water of the eastern Gambia Abyssal Plain, its area of influence seems rather limited. It is not visible in the Kane Gap section (Fig. 18), north of the Cape Verde Ridge along the 25°W section (Fig. 12), nor anywhere along the 35°W (Fig. 9) and 24°N sections (Fig. 21). It does appear on the eastern part of the 16°N section atop the Cape Verde Ridge (Fig. 22) where it intersects the 29°W section (Fig. 12): the low oxygen feature extends from about 32°W eastward to the continental rise where the layer intersects the sea floor. The "adjusted" oxygen values of the 16°N section are open to question, however.

5) Poleward flow along the Mid-Atlantic Ridge

To conclude our discussion of the impact of the Vema on the abyssal water over the Gambia Abyssal Plain, we return to the northwest quadrant of the plain. The eastward flow across the *Knorr* section immediately north of the Vema was described earlier: descending isotherms northwards across the two station pairs 80–75–74. Transports are very uncertain because of the rough topography. Perhaps the main lesson of Fig. 15 is that there is monotonic shear all the way up through the Deep Water, so that there is a stronger dependence of the Bottom Water transport on the mid-depth reference level than is the case within the Vema (Fig. 11).

North of this region of poorly quantified eastward Bottom Water transport, the *Knorr* section (Fig. 9) shows the Deep and Bottom water isotherms reversing slope and rising northwards (stations 70–74) to the Cape Verde Ridge. Isotherms descend a bit and then recover for stations 66–70, so that transports for the extended group 66–74 differ little from those of the smaller group 70–74. We will continue the discussion using the extended group. The net northward rise of isotherms across this group defines a poleward flow of Bottom Water along the flank of the Mid-Altantic Ridge towards the northwestern corner of the plain. The effect of this flow is apparent in the bottom temperature distribution (Fig. 13): the northward bulge of the 1.76°, 1.78°, and 1.8°C isotherms north of the Vema.

Estimating Bottom Water transport for this poleward flow is difficult. The effect of correcting for abyssal bathymetry on the transports is less dramatic here (Fig. 23) than it was for the eastward flow (Fig. 15). But the strong dependence on the reference level remains and is problematic. If cold reference levels are chosen to keep the Bottom Water transport as small as that exiting over the Vema sill, then the overlying Deep Water flows oppositely to the Bottom Water. If the reference level is raised to cause the Deep Water to move in the same direction as the Bottom Water, then the Bottom Water transports become rather large.

Our best estimate at this station group of the current's Bottom Water transport is 1.8 to 3.9 ($\times 10^6$ m^3 s^{-1}). This estimate was computed with bottom triangle transports reduced to account for topographic blocking and reference levels ($2.2° < \theta < 2.6°$C) such that the lower Deep Water ($2.0° < \theta < 3.0°$C) moves in the same direction as the Bottom Water ($\theta < 2.0°$C) (transport reference level dependence and unadjusted transports for the expanded group of stations, 66 to 74, is shown in Fig. 23). Figure 4 includes a transport of 1.9×10^6 m^3 s^{-1} corresponding to the regional reference level 2.2°C.

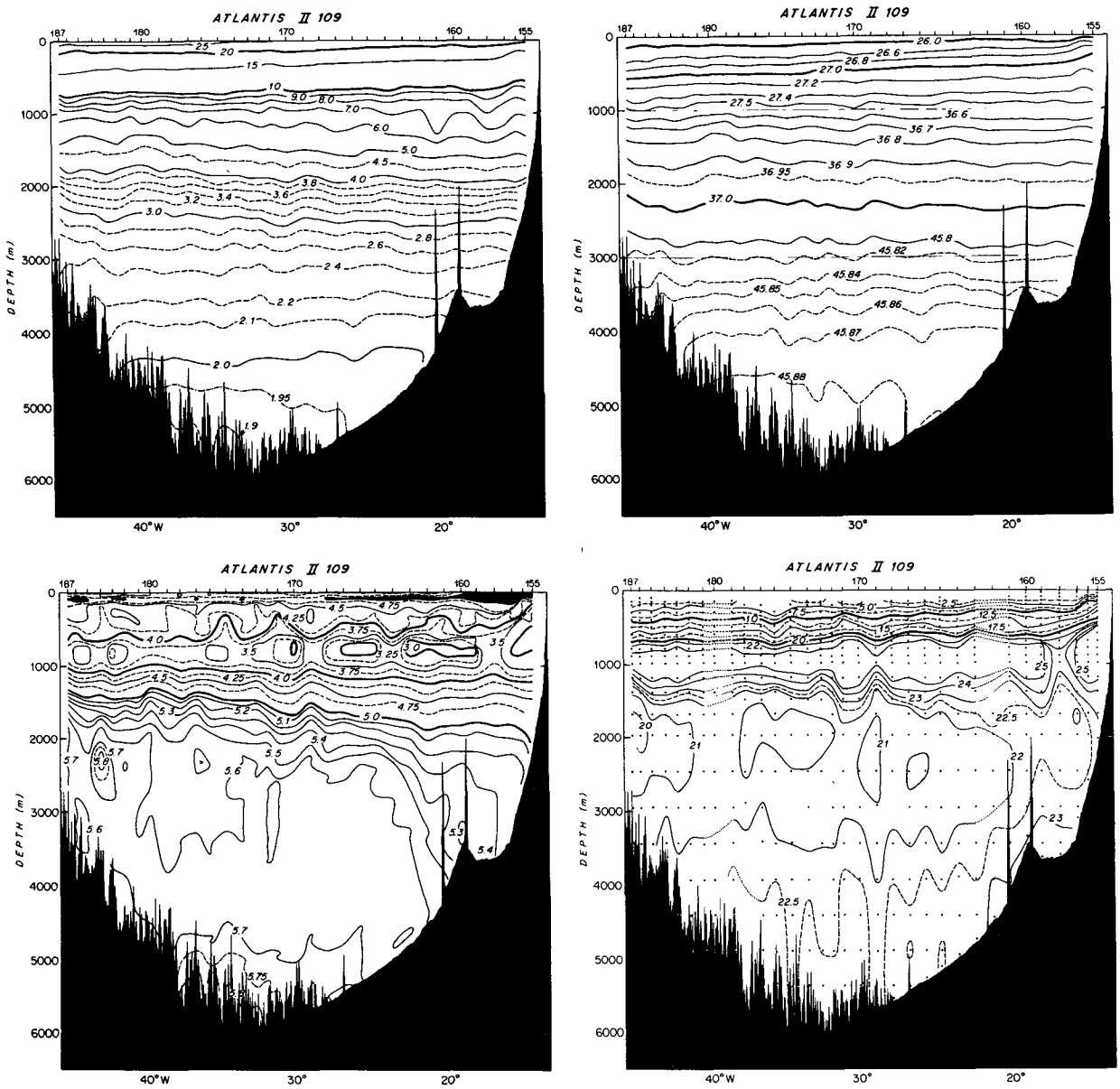

FIG. 21. Property distributions along the 1981 *Atlantis II* zonal section near 24°N (Fig. 3, and Roemmich and Wunsch 1985). (a) Potential temperature (°C). (b) Density parameters σ_0, σ_2, and σ_4 (g kg^{-1}). (c) Dissolved oxygen (ml l^{-1}). (d) Nitrate (μmol l^{-1}).

d. Abyssal circulation 2: South Canary and North Canary basins

1) NORTHWARD FLOW ACROSS THE CAPE VERDE RIDGE

Bottom Water from the Vema appears to flow northward across the Cape Verde Ridge into the South Canary Basin, as can be seen in the cold ($\theta < 1.8$°C) water that extends northward along the Mid-Atlantic Ridge flank and terminates atop the Cape Verde Ridge at about 38°W (Fig. 9a). Situated more or less on top of the Cape Verde Ridge, the IGY 16°N sections of temperature, oxygen (Fig. 22), and phosphate (not shown due to low quality) show a western-intensified, low-temperature, high-oxygen, low-phosphate bubble of Deep and Bottom Water at and west of 38°W consistent with northward flow of Vema-influenced water there.

Data is lacking to determine with any precision the extent of cold water penetration into the South Canary Basin and the temperature of the coldest flow across

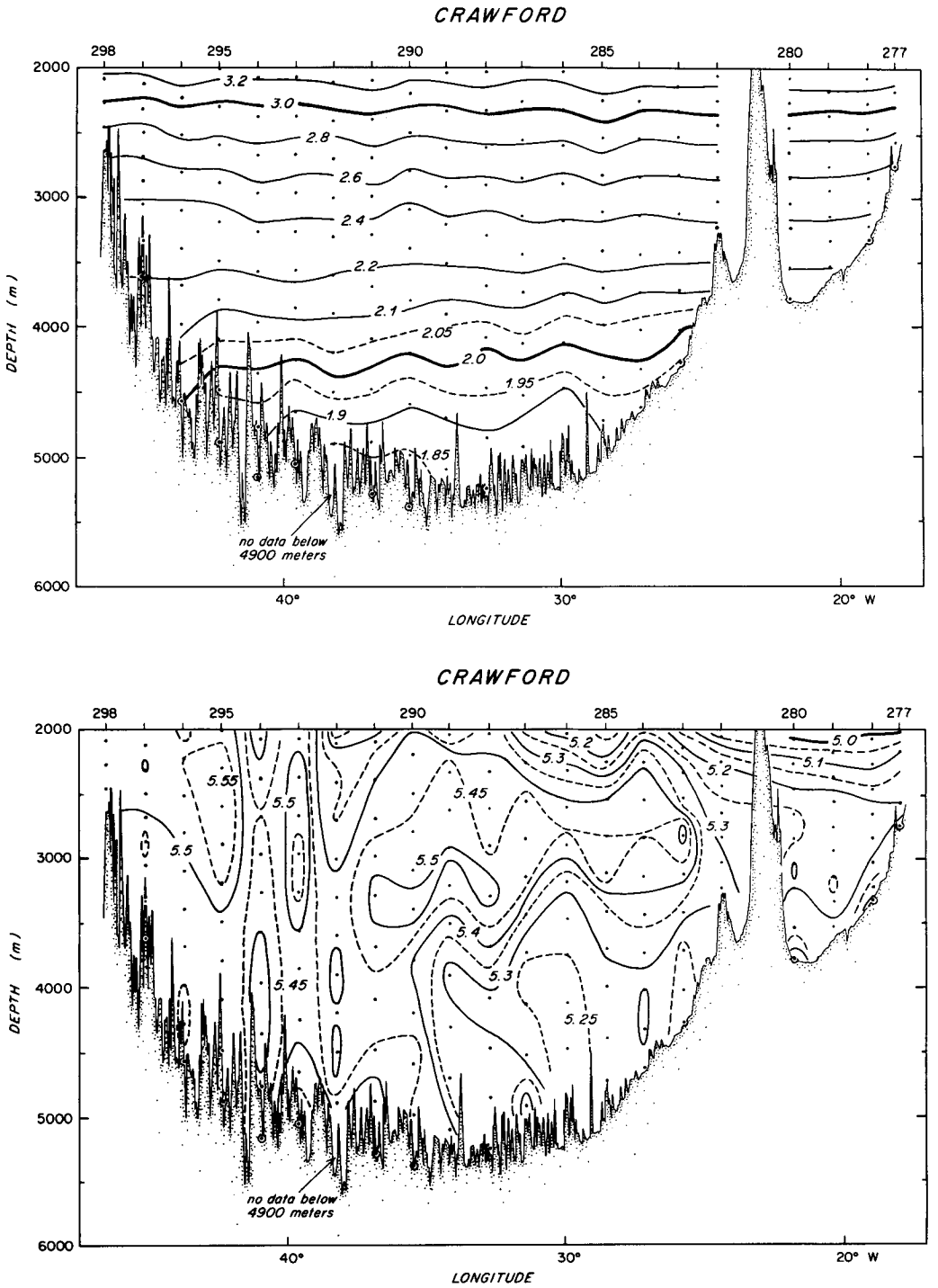

FIG. 22. Property distributions along the 1957 *Crawford* zonal section near 16°N (Fig. 3, and Fuglister 1960). (a) Potential temperature (°C). (b) Dissolved oxygen (ml l^{-1}). This is contoured using the original data. Worthington recommends multiplication by 1.048 to correct observations of this period made at WHOI for systematic error. This can be approximated by adding 0.25 to the label contour values.

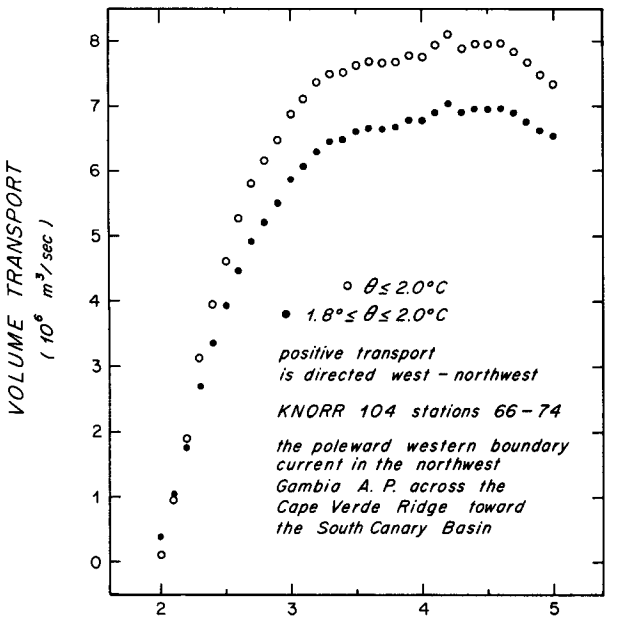

FIG. 23. Transport of water as a function of the assumed potential temperature of an isothermal "level" of no motion. *Knorr*-104 section defining the west–northwest flow from the northwestern Gambia Abyssal Plain across the Cape Verde Ridge into the southwestern South Canary Basin (Figs. 8 and 9).

the Cape Verde Ridge. The coldest bottom temperatures at the Cape Verde Ridge are probably found in a >5500 m deep and 70 km wide gap at 38°W, visible at station 292 in Fig. 22. Unfortunately, no observations are available from the depths of this feature (station 291 sampled to only 4900 m); our best guess is $\theta_B \leq 1.75$°C, based on a station just to the southwest ($\theta_B = 1.75$°C at 5124 m and 15°39'N, 38°35'W; Reid, personal communication 1988). North of the ridge, there is no data in the immediate neighborhood of the 38°W gap, and three of the four stations defining the θ_B contouring are very old: two *Rambler* stations listed by Wüst (1933) from 1895, and *Meteor* 283 from 1927.

2) South Canary Basin Bottom Water circulation

The Mid-Atlantic Ridge axis on the western side of the South Canary Basin curves from a north–south orientation at 24°N to east–west at 30°N. The basin's deep western boundary current is crossed nearly at right angles by both a 24°N zonal section and also by a 35°W meridional section (respectively, 1981 *Atlantis II* 109 shown in Fig. 21 and *Knorr* 104 shown in Fig. 9). These sections cross the basin interior and intersect in the southern basin near *Knorr* station 56 and *Atlantis II* station 176 (Fig. 3).

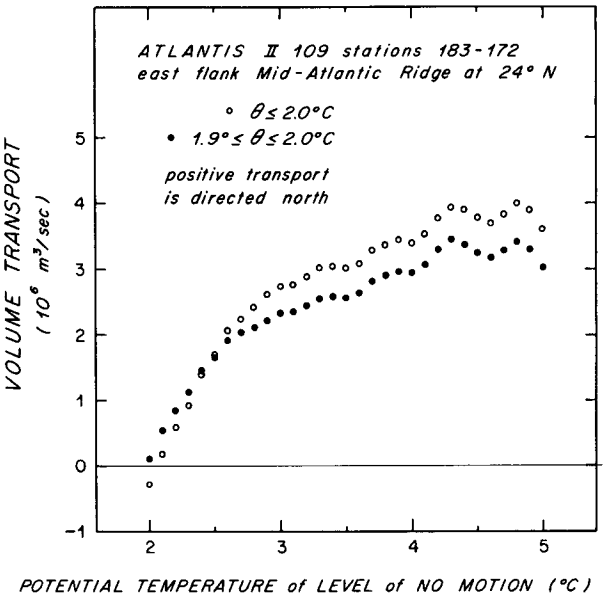

FIG. 24. Transport of water as a function of the assumed potential temperature of an isothermal "level" of no motion. *Atlantis II*-109 section defining the boundary current along the east flank of the Mid-Atlantic Ridge at 24°N (Fig. 21).

A Gambia Abyssal Plain origin for the cold ($\theta < 1.9$°C) water of the western South Canary Basin (*Knorr* stations 54 to 59 and *Atlantis II* stations 174 to 179) is suggested by its high oxygen (>5.8 ml l^{-1})

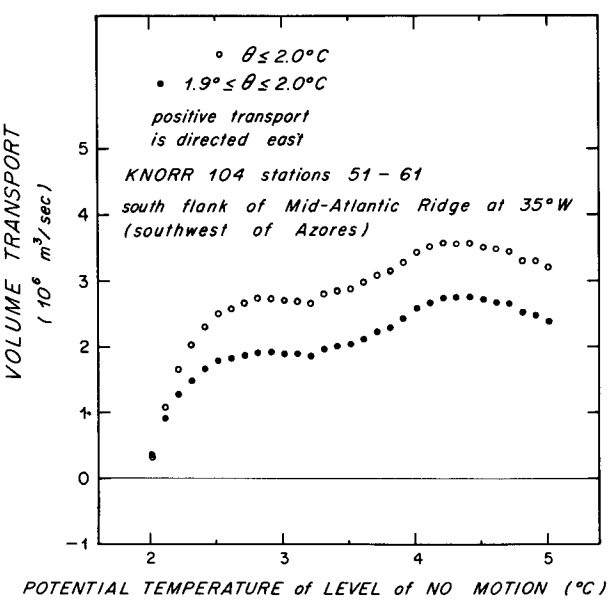

FIG. 25. Transport of water as a function of the assumed potential temperature of an isothermal "level" of no motion. *Knorr*-104 section defining the boundary current along the east flank of the Mid-Atlantic Ridge at 35°W (Fig. 9). The ridge is oriented nearly east–west at this location (Fig. 3).

and high stratification (see isopycnal spacing, Figs. 9b and 21b); both are higher than levels anywhere else in the basin at these temperatures. A flow path along the Mid-Atlantic Ridge flank connects the more northern high-oxygen, high-stratification pool and the Vema water (*Knorr* stations 70 to 80) of the 35°W section; their apparent isolation from each other is an artifact of the section orientation.

The South Canary Basin deep western boundary current transport at 24°N (Fig. 24) is 0.9 to 1.7 × 10^6 m^3 s^{-1} after adjusting for topographic blocking effects, for cold (<2.0°C) water and our preferred reference level range, 2.2° ≤ θ ≤ 2.5°C. As in the northwest Gambia Abyssal Plain, the colder reference levels have been excluded by requiring lower Deep Water to flow with Bottom Water. The analogous transport ranges at 35°W [Fig. 25, 1.3 to 1.8 (×10^6 m^3 s^{-1})] are remarkably similar, overlapping to within about 0.5 × 10^6 m^3 s^{-1}. All these transports are, however, rather uncertain due to the very rough topography. There is, however, less shear in the Deep Water, and hence less dependence of the Bottom Water transport on the temperature of reference levels than was found in the northwestern Gambia Abyssal Plain. In Fig. 4 we assign a transport of 1.1 × 10^6 m^3 s^{-1} to this area of the South Canary Basin.

The deep western boundary current transport is smaller by roughly 1 × 10^6 m^3 s^{-1} in the South Canary than in the Gambia Abyssal Plain and crossing Cape Verde Ridge (Fig. 23). One would expect boundary current transport streamlines to turn eastward into the interior circulation, and it is also possible that water leaks into the western trough at the Kane Fracture Zone at 24°N as Metcalf (1969), first suggested on the basis of high silicate levels in the Bottom Water west of the ridge.

3) Bottom Water flow into the North Canary Basin

Poleward flow of Bottom Water along the ridge flank is even more evident in the southward rising of deep isotherms at about 25°N, 30°W, on two occupations of the beta-triangle eastern side (Fig. 26; Armi and Stommel 1983; Behringer et al. 1983). Further continuation of Bottom Water transport up into the North Canary Basin is suggested by the western-intensified

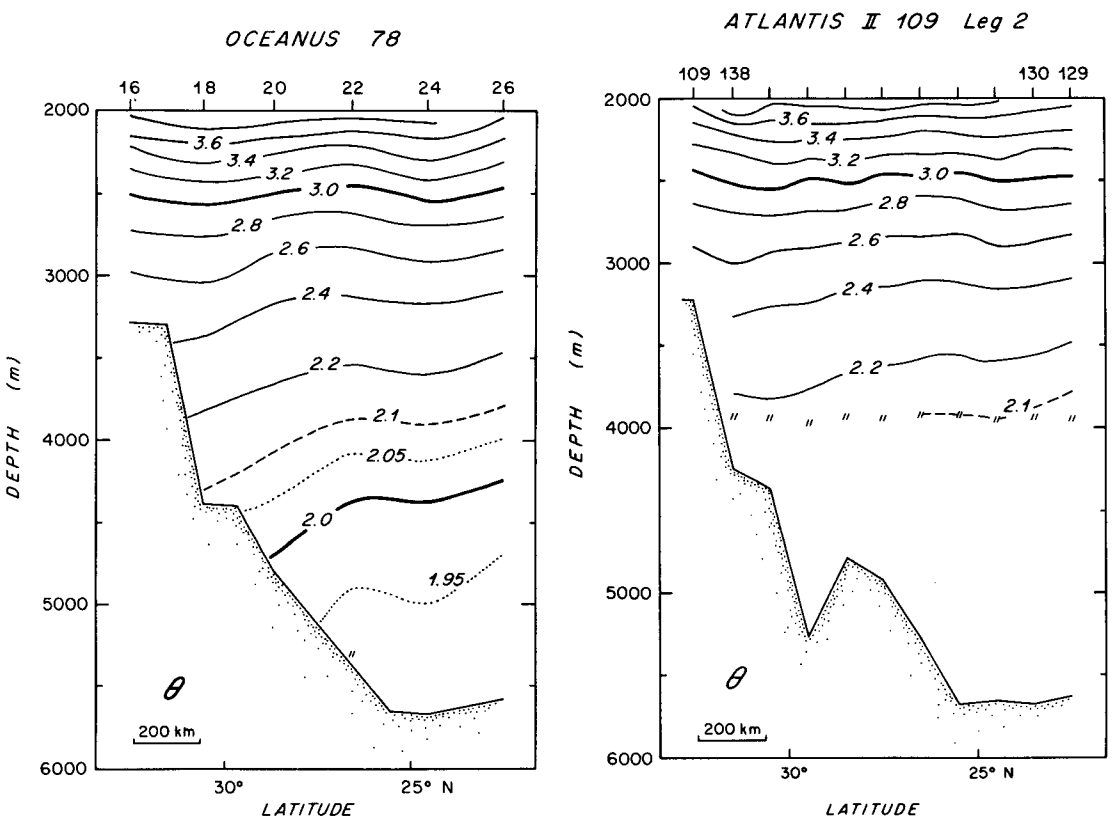

FIG. 26. Deep potential temperature distributions along two occupations of the eastern side of the "β-triangle" [Armi and Stommel 1983, data from Behringer et al. (1983), location given by *Oceanus* 78 station data (Fig. 3); *Atlantis II* is same location at half the station spacing.]

northward intrusion of the 1.94° and 1.96°C θ_B contours (Fig. 13b).

Deep isotherms rise eastward across the North Canary Basin at 36°N [Fig. 27, showing a segment of the Roemmich and Wunsch (1985) 36°N section]. The deep flow evidently northward continues here, but as noted by Saunders (1987), with eastern intensification. The coldest water, now with $\theta \geq 2.0$°C continues to have elevated oxygens, near 5.8 ml l^{-1} indicative of its immediate origin in the western South Canary Basin. Evidence for continued eastward concentration of the northward flow of the Vema-originating waters to 50°N is discussed in McCartney (1991).

The North Canary Basin is bounded to the north by the East Azores Fracture Zone scarps (Fig. 1). Two narrow passages with depths > 4500 m cut through to the north at 19°30'W and 16°W (Discovery Gap), judging from the Searle et al. chart. According to Saunders (1987), geostrophic northward cold transport through the passages is 0.55×10^6 m^3 s^{-1}, relative to a reference level of 2.3°C based on his analysis of the regional circulation. The transport consists of water with temperatures between slightly above 2.0°C (the coldest water here) and 2.05°C; about two-thirds of the reported transport comes through the Discovery Gap.

The northward transport of water colder than 2.05 through the passages agrees well with the net transport at 36°N (Fig. 27, *Atlantis II* stations 76 to 86) of 0.58×10^6 m^3 s^{-1}, computed using Saunders' temperature reference level. This value is included in Fig. 4 as a dashed arrow indicating horizontal flow across the 2.0° isotherm. At 36°N, the northward transport has shifted to the eastern side of the basin: the transport field consists of about 0.83×10^6 m^3 s^{-1} flowing north in the east (stations 81 to 86) and about 0.37×10^6 m^3 s^{-1} flowing south in the west (stations 76 to 81). A near-bottom low nitrate pocket (stations 76–77) indicates that the southward flow carries northern source characteristics.

Saunders suggested that the eastern-intensified current is the upstream boundary current supplying a dense overflow. We offer an alternative rationalization. A Stommel–Arons-type basin can exhibit an east–west contrast of water types north of a critical latitude with:

- a northward-flowing western boundary current north of the low-latitude source up to the critical latitude where the last source streamline peels off into the interior;
- a southward-flowing western boundary current poleward of the critical latitude;
- south of the critical latitude, an interior filled with streamlines originating from the northward-flowing boundary current;
- north of the critical latitude, the western interior streamlines emerge from the southward-flowing boundary current; and
- north of the critical latitude, the eastern interior streamlines originate from the northward flowing boundary current somewhere south of the critical latitude.
- The relative proportion of southern source water north of the critical latitude decreases with latitude.

In this scenario, with a critical latitude near 30°N, the Vema Bottom Water influence would be restricted to the east north of 30°N.

4. Conclusions

We have confirmed (with new high-quality CTD hydrographic transects, Fig. 3), Mantyla and Reid's inference that eastward flow through the Vema determines the abyssal water mass characteristics of the northeastern Atlantic basins (Gambia Abyssal Plain, South Canary Basin, and North Canary Basin), and laid to rest the idea that Romanche-derived waters play a significant role there. The near-bottom temperature field (Fig. 12) shows water emanating from Vema and spreading along the southern boundary of the plain as far as Kane Gap, though none flows south there, and along the eastern flank of the Mid-Atlantic Ridge as far north as the North Canary Basin. Neither northward nor southward flow colder than 2.0°C occurs at Kane Gap to connect the water masses of the northeastern Atlantic basins to the tropical Atlantic basins.

We have estimated geostrophic transport colder than 2.0°C at the Vema exit, as seen in our 1983 high-resolution station line, to be 2.08 to 2.32 ($\times 10^6$ m^3 s^{-1}) relative to a 2.17° to 2.43°C reference level. This range of reference levels was chosen because it produces Vema flows consistent with nitrate extrema and sensible northeastern basin western boundary current transports. These new transport values are much higher than all previous Vema transport estimates, but these older values were either limited to colder waters (Vangriesheim 1980; Eittreim et al. 1983) or result from model runs that significantly misrepresent the mean tracer characteristics of the Vema cold water flow (Schlitzer 1987). It appears that the transport of cold water through the Vema would be significantly less if the Bottom Water of the western trough were not "transposed" onto the western flank of the Mid-Atlantic Ridge; the dynamics of this interesting relationship are explored elsewhere (Speer and McCartney 1991). We have also confirmed Heezen et al.'s (1964) prediction of a secondary sill for the Vema, to elevate the temperature of the exiting water to the warmer values observed in the Gambia Abyssal Plain.

Vema influence spreads through the eastern Atlantic basins by way of a system of deep boundary currents (Fig. 4). Just outside the Vema exit, we found the exit flow to turn from almost northward to about eastward, then to bifurcate into a poleward flow along the flank of the Mid-Atlantic Ridge and an eastward flow along

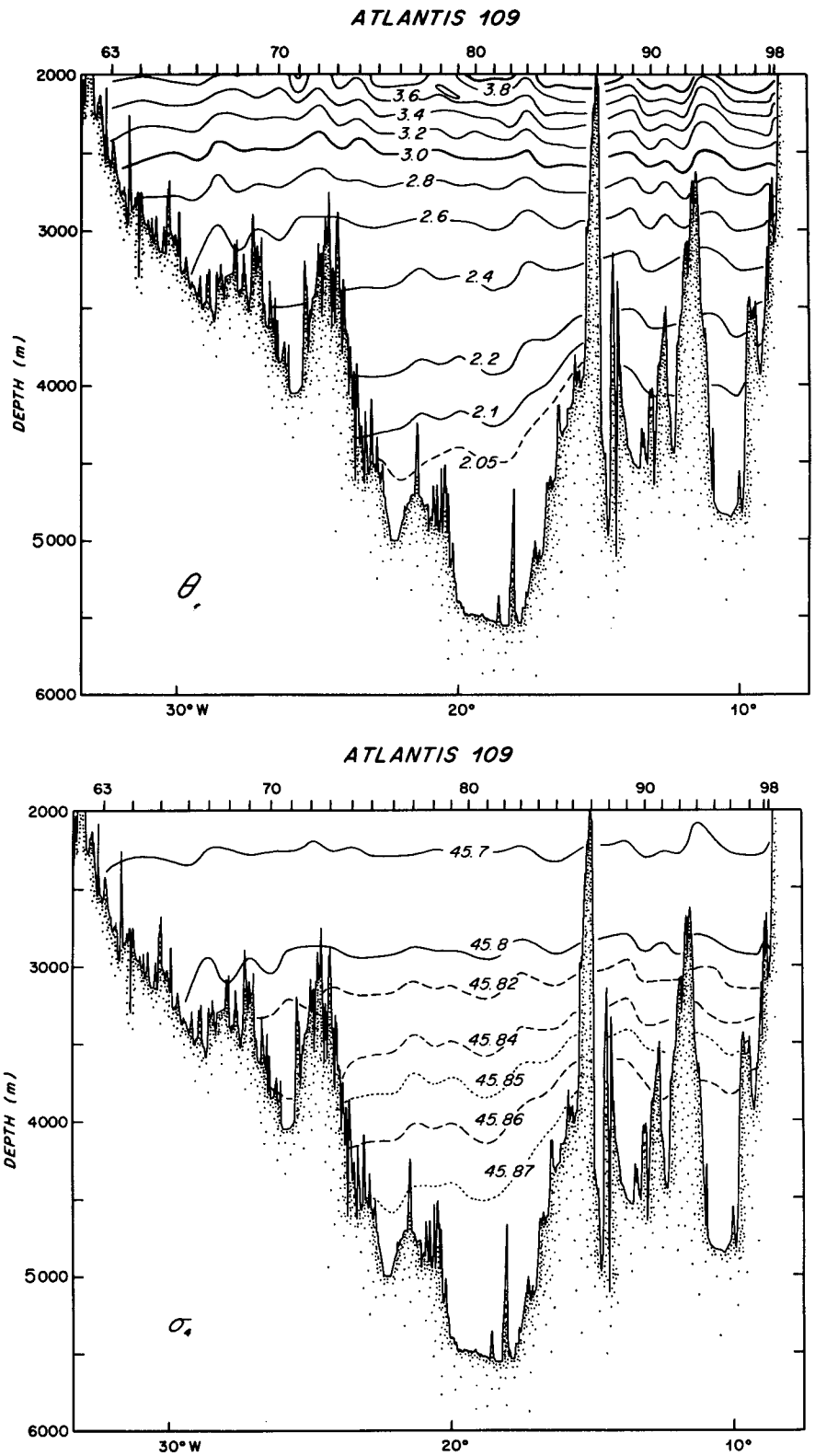

FIG. 27. Deep property distributions along the 1981 *Atlantis II* zonal section near 36°N (Fig. 3 and Roemmich and Wunsch 1985). (a) Potential temperature (°C). (b) Potential density parameters σ_4 (g kg^{-1}).

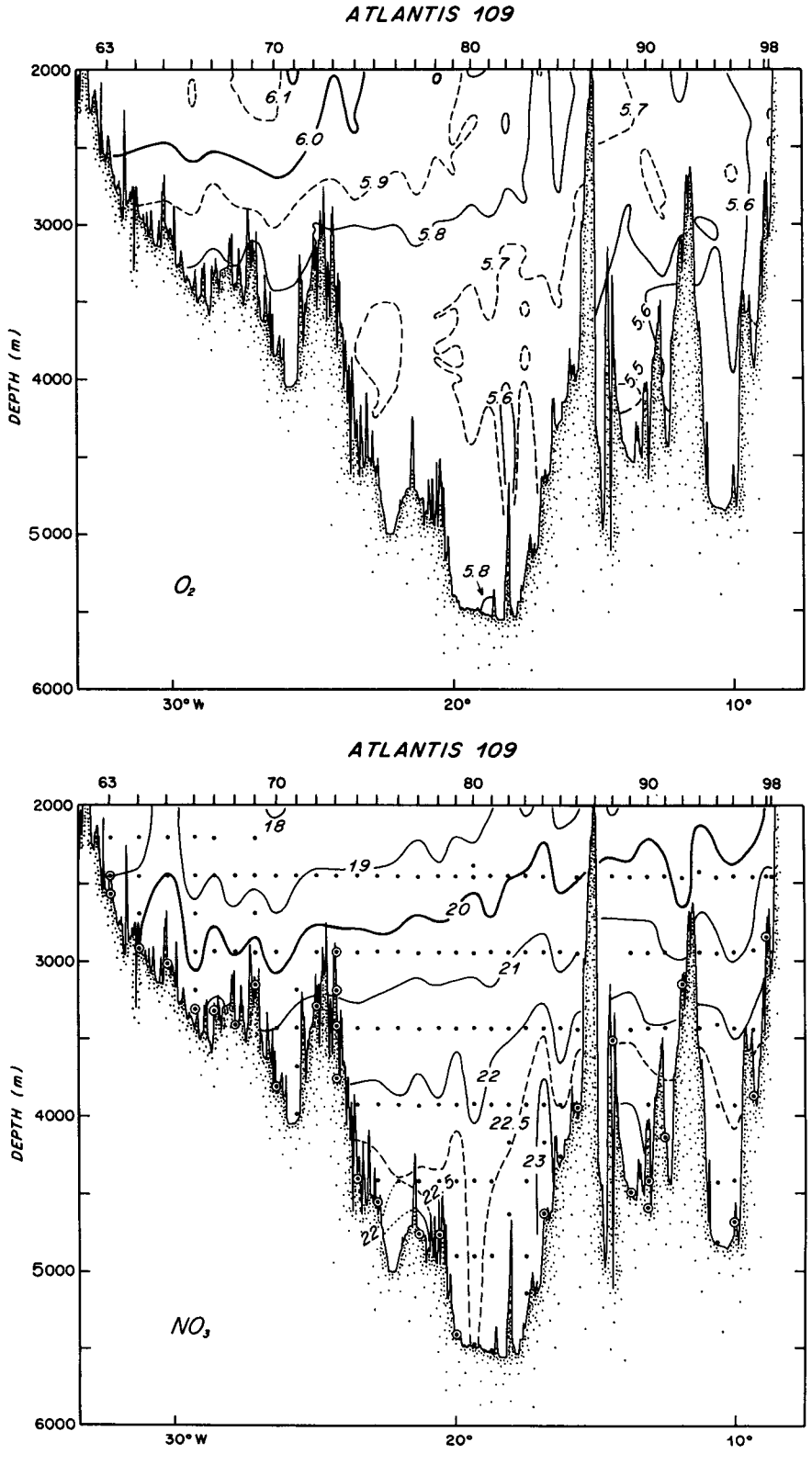

FIG. 27. (*Continued*) (c) Dissolved oxygen (ml l^{-1}). (d) Nitrate (μmol l^{-1}).

the southern boundary of the Gambia Abyssal Plain. It has been argued that the dynamics of the south plain eastward flow could be those of a topographically channeled jet or of southern boundary current of the plain's abyssal circulation, or a combination of the two (in principal, the eastward flow could feed southward Kane Gap throughflow, but the observations indicate that the throughflow is negligible).

Below 2.0°C, the eastern Gambia Abyssal Plain is a cul-de-sac occupied by cyclonically turning flow. The coldest flow evidently returns westward relatively directly, incurring little change in its nitrate and oxygen values, while the warmer water seems to swing farther east before turning, in the process gaining nitrate and losing oxygen in significant amounts; these tracer changes may be due to greater aging along a longer flow path, or to contact with organic sediments on the continental rise beneath the West African coastal upwelling regime.

The northwestern Gambia Abyssal Plain contains a strong cyclonic turning flow, with an east limb carrying the Vema outflow onto the plain, and the north branch of that flow's bifurcation turning cyclonically to flow northwestward crossing the Cape Verde Ridge and supplying Bottom Water to the South Canary Basin. Continued poleward flow along the western boundary—the east flank of the Mid-Atlantic Ridge—is observed in the South Canary Basin. It switches to the east side of the North Canary Basin north of 30°N, which may reflect the intrusion of southward boundary current flow to 30°N.

Acknowledgments. The authors would like to thank Ruth Curry and Teresa Turner for their excellent work in bringing together the diverse datasets and the numerical and replical digestions of them that form the basis for our analysis. The participants of the many *Oceanus, Knorr* and *Atlantis II* cruises, science and crew, have performed long and well for the senior author, and he thanks them for their efforts. We especially acknowledge Dean Roemmich and Mindy Hall for the early access to their 1989 "10°N" *Oceanus* section, which so greatly improved the resolution to Fig. 13—and our confidence in the contouring! Jan Zemba made available to us her transport programs incorporating a novel method for estimating the "bottom triangle" contributions. The long assembly task for this manuscript was handled in smooth fashion by Doris Haight, Karin Bohr, and Anne-Marie Michael. Comments by Bruce Warren, Kevin Speer, and Ruth Gorski helped us recognize and clear up various murky points. This work was funded by the National Science Foundation under Grants OCE 78-22223, OCE 86-01017, and OCE 86-14486 and by the Office of Naval Research under Contact N00014-82-C-0019, NR 083-004.

REFERENCES

Armi, L., and H. Stommel, 1983: Four views of the North Atlantic subtropical gyre. *J. Phys. Oceanogr.*, **13,** 828–857.

Bainbridge, A. B., 1981: GEOSECS Atlantic Expedition, Volume 1, Hydrographic Data 1972–1973, U.S. Government Printing office, Washington, D.C. 121 pp.

Behringer, D. W., G. P. Knapp, R. J. Stanley and H. M. Stommel, 1983: Hydrographic station data of five surveys of the beta-triangle in the eastern North Atlantic, 1978–1981. Woods Hole Oceanographic Institution Tech. Rep. 83–24, 246 pp.

Chan, L. H., D. Drummond, J. M. Edmond and B. Grant, 1977: On the barium data from the Atlantic GEOSECS Expedition. *Deep-Sea Res.*, **24,** 613–649.

Drygalski, E. von, 1904: *Zum Kontinent des eisigen Südens.* Georg Reimer, Berlin, 668 pp.

Egloff, J., 1972: Morphology of ocean basin seaward of Northwest Africa: Canary Islands to Monrovia, Liberia. *Bull. Amer. Assoc. Petrol. Geol.*, 684–706.

Eittreim, S. L., P. E. Biscaye and S. S. Jacobs, 1983: Bottom-water observations in the Vema Fracture Zone. *J. Geophys. Res.*, **88,** 2609–2614.

Fuglister, F. C., 1960: Atlantic Ocean atlas of temperature and salinity profiles and data from the International Geophysical Year of 1957–1958. Woods Hole Oceanographic Institution Atlas Series 1, 209 pp.

Heezen, B. C., R. D. Gerard and M. Tharp, 1964: The Vema Fracture Zone in the equatorial Atlantic. *J. Geophys. Res.*, **69,** 733–739.

Hobart, M. A., E. T. Bunce and J. G. Sclater, 1975: Bottom water flow through the Kane Gap, Sierra Leone Rise, Atlantic Ocean. *J. Geophys. Res.*, **80,** 5083–5088.

Krause, D. C., 1964: Guinea Fracture Zone in the Equatorial Atlantic, *Science,* **146,** 57–59.

Mantyla, A. W., and J. L. Reid, 1983: Abyssal characteristics of the World Ocean waters. *Deep-Sea Res.*, **30,** 805–833.

McCartney, M. S., 1991: Recirculating components to the Deep Boundary Current of the Northern North Atlantic, *Progress in Oceanograph.* submitted.

McCartney, M. S., and K. G. Speer, 1991: The distribution and circulation of the Antarctic Bottom Water in the western North Atlantic Ocean, *J. Phys. Oceanography,* submitted.

Metcalf, W. G., 1969: Dissolved silicate in the deep North Atlantic. *Frederick C. Fuglister Sixtieth Anniversary Volume. Deep-Sea Res.*, **16**(Suppl.), 139–145.

——, B. C. Heezen and M. C. Stalcup, 1964: The sill depth of the Mid-Atlantic Ridge in the equatorial region. *Deep-Sea Res.*, **11,** 1–10.

Östlund, H. G., W. S. Broecker and D. Spencer, 1987: GEOSECS Atlantic, Pacific and Indian Ocean Expedition, Vol. 17. Shore-based data and graphics. U.S. Govt. Printing Office, Washington, D.C., 200 pp.

——, and C. Grall, 1987: Transient Tracers in the Ocean. North and Tropical Atlantic Tritium and Radiocarbon. Tritium Laboratory Data Report 16, University of Miami, Rosenstiel School of Marine and Atmospheric Science, Miami, Florida. 277 pp.

Roemmich, D., and C. Wunsch, 1985: Two transatlantic sections: Meridional circulation and heat flux in the subtropical North Atlantic Ocean. *Deep-Sea. Res.*, **32,** 619–664.

Saunders, P. M., 1987: Flow through Discovery Gap. *Deep-Sea Res.*, **17,** 631–643.

Schlitzer, R., 1987: Renewal rates of east Atlantic Deep Water estimated by inversion of ^{14}C data. *J. Geophys. Res.*, **92,** 2953–2969.

Scripps Institution of Oceanography, 1986: Shipboard Physical and Chemical Data Report, Transient Tracers in the Ocean Tropical Atlantic Study, 1 December, 1982–18 February 1983. Scripps Institution of Oceanography, University of California, SIO Ref. 86-16, 300 pp.

Searle, R. C., D. Monahan and G. L. Johnson, 1982: General Bathymetric Chart of the Oceans, Chart 5.08, International Hydrographic Organization, published by the Canadian Hydrographic Service, Ottawa.

Speer, K. G., and M. S. McCartney, 1991: Bottom Water circulation in the western North Atlantic. *J. Phys. Oceanogr.*, in press.

Stommel, H., and A. B. Arons, 1960: On the Abyssal Circulation of the World Ocean—II. An Idealized model of the circulation

pattern and amplitude in Oceanic Basins. *Deep-Sea Res.*, **6**, 217–233.

Tsuchiya, M., L. D. Talley and M. S. McCartney, 1991: An eastern Atlantic section from Iceland southward across the equator. *Deep-Sea Res.*, submitted.

Vangriesheim, A., 1980: Antarctic Bottom Water flow through the Vema Fracture Zone. *Oceanol. Acta*, **3**, 199–207.

Warren, B. A., 1981: Deep water circulation in the world ocean. *Evolution of Physical Oceanography*, B. A. Warren and C. Wunsch, Eds., MIT Press, 6–41.

——, and K. G. Speer, 1991: Deep circulation in the eastern South Atlantic Ocean. *Deep-Sea Res.*, in press.

Worthington, L. V., and W. R. Wright, 1970: North Atlantic Ocean Atlas of Potential Temperature and Salinity in the Deep Water Including Temperature, Salinity, and Oxygen profiles from the *Erika Dan* Cruise of 1962. Woods Hole Oceanographic Institution Atlas Series 2, 24 pp. and 58 plates.

Wright, W. R., 1970: Northward transport of Antarctic Bottom Water in the western Atlantic Ocean. *Deep-Sea Res.*, **17**, 367–371.

Wüst, G., 1933: Schichtung und Zirkulation des Atlantischen Ozeans. Das Bodenwasser und die Gliederung der Atlantischen Tiefsee. *Wissenschaftliche Ergebnisse der Deutschen Atlantischen Expedition auf dem Forschungs—und Vermessungsschiff "Meteor" 1925–1927*, **6**, 1st Part, 1, 106 pp. [*Bottom Water and the Distribution of the Deep Water of the Atlantic*, M. Slessers, translator, B. E. Olson, Ed., 1967, U.S. Naval Oceanographic Office, Washington, D.C. 145 pp.]

——, 1935: Schichtung und Zirkulation des Atlantischen Ozeans. Die Stratosphare. In: *Wissenschaftliche Ergebnisse der Deutschen Atlantischen Expedition auf dem Forschungs—und Vermessungsschiff "Meteor" 1925–1927*, **6**, 1st Part, 2, 180 pp. [*The Stratosphere of the Atlantic Ocean*, W. J. Emery, Ed., 1978, Amerind, 112 pp.]